# The multimodal action of G alpha q in coordinating growth and homeostasis in the *Drosophila* wing imaginal disc

**Vijay Velagala[1, #], Dharsan K. Soundarrajan[1, #], Maria F. Unger[1, #], David Gazzo[1], Nilay Kumar[1], Jun Li[3], Jeremiah Zartman[1,2 *]**

[1] Department of Chemical and Biomolecular Engineering, University of Notre Dame, Notre Dame, IN 46556

[2] Department of Biological Sciences, University of Notre Dame, Notre Dame, IN 46556

[3] Department of ACMS,171 Hurley Hall, University of Notre Dame, Notre Dame, IN 46556[2] Department of Applied and Computational Mathematics and Statistics

[*]Correspondence: jzartman@nd.edu

[#]These authors contributed equally

Keywords: $Ca^{2+}$, Dilp-8, growth control, developmental timing, *Drosophila* wing disc

## Abstract

### Background

G proteins mediate cell responses to various ligands and play key roles in organ development. Dysregulation of G-proteins or $Ca^{2+}$ signaling impacts many human diseases and results in birth defects. However, the downstream effectors of specific G proteins in developmental regulatory networks are still poorly understood.

### Methods

We employed the Gal4/UAS binary system to inhibit or overexpress *Gαq* in the wing disc, followed by phenotypic analysis. Immunohistochemistry and next-gen RNA sequencing identified the downstream effectors and the signaling cascades affected by the disruption of Gαq homeostasis.

### Results

Here, we characterized how the G protein subunit Gαq tunes the size and shape of the wing in the larval and adult stages of development. Downregulation of *Gαq* in the wing disc reduced wing growth and delayed larval development. *Gαq* overexpression is sufficient to promote global $Ca^{2+}$ waves in the wing disc with a concomitant reduction in the *Drosophila* final wing size and a delay in pupariation. The reduced wing size phenotype is further enhanced when downregulating downstream components of the core $Ca^{2+}$ signaling toolkit, suggesting that downstream $Ca^{2+}$ signaling partially ameliorates the reduction in wing size. In contrast, *Gαq*-mediated pupariation delay is rescued by inhibition of $IP_3R$, a key regulator of $Ca^{2+}$ signaling. This suggests that Gαq regulates developmental phenotypes through both $Ca^{2+}$-dependent and $Ca^{2+}$-independent mechanisms. RNA seq analysis shows that disruption of Gαq homeostasis affects nuclear hormone receptors, JAK/STAT pathway, and immune response genes. Notably, disruption of Gαq

48 homeostasis increases expression levels of Dilp8, a key regulator of growth and pupariation
49 timing.

50 **Conclusion**

51 Gαq activity contributes to cell size regulation and wing metamorphosis. Disruption to Gαq
52 homeostasis in the peripheral wing disc organ delays larval development through ecdysone
53 signaling inhibition. Overall, Gαq signaling mediates key modules of organ size regulation and
54 epithelial homeostasis through the dual action of $Ca^{2+}$-dependent and independent mechanisms.

# Abbreviations

**AkhR**: Adipokinetic Receptor

**chinmo**: chronologically incorrect morphogenesis

**DAG**: diacylglycerol

**DAPI**: 4′,6-Diamidino-2-phenylindole dihydrochloride

**DCP**: Cleaved Drosophila Dcp-1 (Asp215) Antibody

**DCP-1**: death caspase-1

**Dpp**: Decapentaplegic

**DUOX**: Dual oxidase

**Eig**: Ecdysone-induced gene

**ER**: endoplasmic reticulum

**ERK**: extra-cellular-signal-regulated protein kinase

**GDP**: guanosine diphosphate

**GO**: Gene Ontology

**GPCRs**: G protein-coupled receptors

**GTP**: guanosine triphosphate

**Gαq O.E.**: G alpha q Overexpression

**Gαq RNAi**: G alpha q RNAi

**Gαq**: G alpha q

**Hh**: Hedgehog

**Hr**: Hormone receptor

**Hsp**: Heat shock protein

**ICWs**: intracellular calcium waves

**Im33**: Immune-induced molecule 33

**IP3**: inositol trisphosphate

**IP3R**: IP3 Receptor

**JNK**: Jun-N-terminal-Kinase

**Lys**: Lysozyme

**MAPK**: mitogen-activated protein kinase

**mthl**: methuselah-like

**NGS**: Normal Goat Serum

**Oatp74D**: Organic anion transporting polypeptide 74D

**PBS**: Phosphate-buffered saline

**Pdk1**: Phosphoinositide-dependent kinase 1

**PH3**: Phospho-Histone H3 (Ser10) Antibody

**PKC**: protein kinase C

**PLC-β**: phospholipase Cβ

**rk**: rickets

**RNA**: Ribonucleic acid

**RNAi**: RNA interference

**Serpin, Spn**: Serin Protease Inhibitor

**Spz**: Spatzle

**upd3**: unpaired3

**Wg**: wingless

## Background

How organs achieve their final size and shape during development is a fundamental question that has long puzzled biologists[1]–[4]. Additionally, the control of size and shape for multicellular systems, including synthetic organoids, is a key consideration for many applications in cell and tissue engineering[5]. Organ size control relies on both intrinsic intra-tissue and extrinsic hormonal growth regulators[6]. Information transfer between external cues and intrinsic signals is essential for maintaining robust physiology. This is achieved, in part, by G-protein coupled receptors (GPCRs), which constitute the largest family of receptors bound to the plasma membrane. GPCRs encode a diverse range of external signals into internal signaling dynamics, thereby modulating diverse physiological processes, including growth and proliferation[7]. Heterotrimeric G proteins form a vital component for the GPCR-mediated signaling cascade[8]–[10]. G proteins are coupled to GPCRs and are known to regulate a wide range of secondary messengers. In addition, G proteins transmit mitogenic signals from hormones and other ligands across the plasma membrane into the cell through its coupled receptors and mediate the cell's response to these signals[9], [11]–[15].

G proteins are ubiquitous in plants and in all animals ranging from *Drosophila* to humans[16]. G-proteins are composed of α, β, and γ subunits that are associated with GPCRs as heterotrimeric complexes (**Fig. 1A**), where each subunit is classified into different families based on their structure and function[11]. For instance, the G*α* subunit is classified into four families: $G\alpha_i$, $G\alpha_s$, $G\alpha_{12/13}$, and *Gαq*. Upon binding of the agonist, the receptor alters its conformation, leading to guanosine diphosphate (GDP) from Gα being exchanged with guanosine triphosphate (GTP)[17]. GTP-bound Gα dissociates from the heterotrimeric complex and activates phospholipase C β (PLC β)[18]. Subsequently, PLC β promotes the hydrolysis of phosphatidylinositol 4,5-biphosphate into second messengers diacylglycerol (DAG) and inositol trisphosphate ($IP_3$)[19].

DAG further activates protein kinase C (PKC)[20], whereas $IP_3$ stimulates the release of $Ca^{2+}$ from the endoplasmic reticulum (ER) (**Fig. 1A, B**) by binding to the $IP_3$ Receptor ($IP_3R$)[19], [21]–[24]. Subsequently, $Ca^{2+}$ binds to a range of proteins to generate diverse cellular responses[25]. More generally, G proteins transduce signals from extracellular cues to generate a range of second messengers such as $IP_3$, DAG, and $Ca^{2+}$, thus providing the framework to develop a broad range of cellular responses[26].

Of note, Gαq serves as a key regulator of diverse biological processes, including growth, glucose transport, actin cytoskeleton regulation, cardiac physiology, and development in various model systems[13], [14], [27], [28]. For example, Gαq is essential for embryonic cardiomyocyte proliferation and cardiac development in mice[29]. Further, mice lacking both *Gαq* and *Gα11* died during embryonic development[29]. Interestingly, mice carrying a mutation for *Gαq* showed retardation in cerebellar maturation, resulting in ataxia and motor discoordination[30]. Also, the loss of *Gαq* and one *Gα11* allele in glial and precursor cells resulted in reduced somatic growth[31]. Moreover, this growth impairment is due to a decrease in the growth hormone release hormone (GHRH), thereby impairing somatotropic cell proliferation and reducing somatic growth. Surprisingly and in contrast, Parton et al. showed that a loss-of-function mouse mutant of *Gαq* in the liver and white adipose tissue results in increased body mass and hyper adiposity[27]. These genetic depletion studies highlight that the *Gαq* is essential for normal development and can act as a growth regulator, with differential phenotypes dependent on cell type. In addition to growth and development, Gαq regulates a diverse set of biological processes. For example, *Gαq* activity is required for insulin-induced glucose transport in adipocytes[13]. Further, the Adipokinetic Receptor (AkhR) functions through the Gαq/Gγ1/Plc21C signaling module to regulate body fat storage in adult *Drosophila*[28]. Mutations in the gene that encodes Gαq subunits have been shown to control skin color and hair color in mouse models[32]. Overall, these studies underscore

the complexity of the diverse biological functions that Gαq performs across a broad range of biological contexts, and in many cases, the downstream pathways remain to be elucidated.

Activating *Gαq* mutations either promotes or inhibits growth based on the level of expression and cellular physiology[15]. For example, expression of the constitutive active form of *Gαq (GαqQ209L)* induced cellular transformation in NIH-3T3 cells[33], [34]. Moreover, Gαq promotes mitogenic activity through its interaction with different mitogen-activated protein kinase (MAPK) signaling pathways[35]–[39]. For instance, Garcia-Hoz et al. reported that the interaction between Gαq and PKCζ is essential for the activation of the extra-cellular-signal-regulated protein kinase (ERK) signaling cascade in cardiac myocytes and fibroblasts[40]. Additionally, activating mutations in *GNAQ,* the gene encoding the Gαq subunit in humans, contribute significantly to the progression of uveal melanoma[32], [41], [42]. However, constitutively active Gαq also can inhibit cell growth in multiple contexts[39], [43], [44]. For example, Kalinec et al. reported that the transfection of *GαqQ209L* (the mutationally active form) in NIH-3T3 cells resulted in fewer colonies and further strongly suggested that high levels of GαqQ209L are cytotoxic to cells[43]. Similar findings are reported by Qian et al., where they observed that the expression of the mutationally active form of Gαq (Gα16) partially inhibited growth in NIH-3T3 cells[45]. Likewise, the expression of an active form of Gα16 inhibits growth in small-cell lung carcinoma cells[39]. Further, this study reported an increase in c-Jun-N-terminal-Kinase (JNK) signaling cascade upon Gα16 expression, thereby suggesting a possible mechanism for growth inhibition. Based on these contrasting effects, it can be inferred that the mutationally active form of Gαq expression regulates growth in a cell-specific manner and subsequently induce different growth phenotypes. However, despite advances in characterizing the functional roles of G proteins in a range of cell types, there is a lack of a general systems-level understanding of how G protein signaling impacts organ growth.

Previously, we have shown that perturbing *Gαq* expression regulates the size of *Drosophila* wings [46]. Further, we identified that the overexpression of wildtype *Gαq* is correlated with the occurrence of intercellular $Ca^{2+}$ waves (ICWs) in *ex vivo* wing disc cultures[46]. Further, Gαq is required for wound-induced $Ca^{2+}$ waves in the pupal notum[47], [48]. Cumulatively, Gαq can either promote or inhibit growth depending on the cellular context and the expression levels. However, the precise molecular mechanisms through which Gαq transduces the growth regulatory signals are not known. This can be primarily attributed due to the wide range of second messengers it activates. For example, the contribution of Gαq-mediated $Ca^{2+}$ signaling toward regulating organ growth parameters, including size and shape, is currently unknown.

To address this question in a well-defined and genetically accessible system, we used the *Drosophila* wing disc to identify the key downstream genes regulated downstream of *Gαq* loss-of-function and gain-of-function perturbations. The *Drosophila* wing imaginal disc is a key model for studying epithelial morphogenesis and signal transduction pathways, including $Ca^{2+}$ signaling[2], [49]–[52]. With the plethora of available genetic tools to generate organ or cell-specific mutants along with the short lifecycle of the *Drosophila*, the wing disc system provides a powerful platform to decode complex signaling mechanisms[53]. The wing disc is invaluable for phenotypic screening in early preclinical studies[54]–[56]. Multiple signaling pathways, such as the Bone Morphogenetic Protein BMP (*Drosophila* Decapentaplegic/Dpp), Wnt (*Drosophila* Wg), and Hedgehog (Hh), coordinate the patterning of epithelial cells and were discovered in the wing imaginal disc[57]–[59]. In *Drosophila*, Gαq plays a key role in regulating neuronal pathfinding[60]. Additionally, it is involved in regulating gut innate immunity through the modulation of DUOX[61]. Also of note, GPCRs are known to regulate metamorphosis by transmitting ecdysone signaling and controlling hormone production through the nuclear hormone pathway[62]–[66]. Altogether, these studies have established different functional roles assumed by Gαq in *Drosophila*. However,

the organ-specific role of Gαq in the growth regulation of peripheral non-neural organ development is relatively less studied.

Here, we combined genetic, phenotypic, and transcriptomic analysis to map the phenotypic consequences of perturbing Gαq homeostasis during organ development to downstream biological processes and pathways. Organ size regulation extensively relies on robust coordination between growth rate and developmental time. We show that *Gαq* perturbations affect both the wing growth and the larval-to-pupal transition time, thereby affecting the final wing size. Our RNA-seq analysis confirms that Gαq modulates key signaling events that regulate growth and developmental time. Thus, Gαq orchestrates the final wing size by interacting with key components of the signaling cascades regulating growth and developmental timing. Additionally, we investigated whether suppressing Gαq-mediated calcium signaling suppresses the reported phenotypes. We found that suppressing calcium signaling components downstream of *Gαq* overexpression suppressed the pupariation delay and further decreased growth. These results suggest that the balance of Gαq regulation of growth through $Ca^{2+}$-dependent and $Ca^{2+}$-independent mechanisms determine the net phenotypic consequences of perturbed Gαq activity during wing development. Overall, this study highlights the multimodal action of the Gαq in balancing growth through the dual action of its protein-protein interactions and secondary messenger regulation and provides a potential mechanism that explains the differential growth outcomes across biological contexts.

# Results

## Gαq homeostasis is necessary for optimal organ size

Gαq signaling has been demonstrated to be essential for the initiation of $Ca^{2+}$ waves in wounded tissues[48]. In addition, our previous study showed that *Gαq* overexpression leads to the formation of intracellular calcium waves (ICWs) in the wing disc pouch cells cultured *ex vivo*[25], [46]. Here, we confirmed this result *in vivo* by imaging larva co-expressing both GCaMP6f and *Gαq* in the wing disc (**Fig. 1C, D**). Both *ex vivo* and *in vivo* imaging confirmed that the *Gαq* expression in the wing disc leads to the formation of regular and repeating ICWs.

Either overexpression or RNAi-mediated inhibition of *Gαq* in the wing disc pouch cells leads to reduced adult wing size, but it is unknown which downstream growth regulatory pathways might be impacted[46], [67]. To further characterize the roles of Gαq in regulating organ growth, we extended and confirmed our phenotypic analysis by testing the impact of *Gαq* perturbation using additional Gal4 drivers, including nubbin-Gal4, MS1096-Gal4, and C765-Gal4. The reported experiments utilize a binary expression system based on the expression of the yeast Gal4 transcription factor, which is driven by a tissue-specific promoter[53]. Consequently, analysis with multiple Gal4 drivers helps to compare the impact of a given Gal4 line. We next quantified the phenotypic consequences for both overexpression and knockdown of Gαq levels. First, we measured the average wing size for the control crosses of each Gal4 line expressing $RyR^{RNAi}$, a control construct that has no known phenotype and targets a gene with no known expression in the wing disc[67] (**Fig. 2A-C**). Next, we knocked down *Gαq* with RNAi constructs using multiple Gal4 drivers (**Fig. 2D-F**). Interestingly, *Gαq* knockdown under the control of the nubbin-Gal4 driver leads to a failure in wing expansion **(Fig. 2D)**. However, the other Gal4 drivers led to relatively normally patterned wings with reduced wing size **(Fig. 2E, F, J)**. This phenotypic variance for

different Gal4 drivers may be attributed to the variation in the spatial-temporal expression patterns of the Gal4 drivers. For instance, MS1096-Gal4 is expressed strongly in the dorsal region of the wing disc pouch during larval and prepupal stages[68], [69], whereas the C765-Gal4 driver is uniformly active in the larval wing disc from the second instar onwards[70]. The protein product of the *nubbin* gene is present from the early second instar onwards but strongly expressed in the third instar discs[71]. Next, we overexpressed *Gαq* in the wing disc using the Gal4 drivers mentioned above. Interestingly, we observed a reduction in the wing size for all the Gal4 drivers. Overexpression of *Gαq* with the MS1096-Gal4 driver showed a smaller wing size when compared with nubbin-Gal4 and C765-Gal4 drivers (**Fig. 2J**). Thus, these results indicate that Gαq homeostasis is essential for normal wing disc growth. Notably, either downregulation or upregulation reduces the final wing size. Further, the severity of the phenotype associated with *Gαq* downregulation varies depending on the Gal4 driver used for the transgenic expression of $Gαq^{RNAi}$.

## Inhibition of $Ca^{2+}$ signaling enhances *Gαq* overexpression phenotypes

Next, we investigated the role of Gαq mediated calcium signaling towards the growth inhibition caused by *Gαq* overexpression. Our previous findings demonstrated that the downregulation of $Ca^{2+}$ signaling components using the MS1096-Gal4 driver resulted in a size reduction of the adult wing[67]. To confirm this, we downregulated the $Ca^{2+}$ signaling components, including *small wing* ( *sl: a homolog of PLCγ)*[72] and *$IP_3R$*, using a C765-Gal4 driver (**Fig. 3A, E, G, I**). The release of $Ca^{2+}$ from ER to the cytoplasm is dependent on the binding of inositol trisphosphate ($IP_3$) to the inositol trisphosphate receptor ($IP_3R$). Further, $IP_3$ is produced by PLC through the hydrolysis of Phosphatidylinositol 4,5-bisphosphate (PIP2). Thus, a major mode of $Ca^{2+}$ signaling relies on $IP_3$ and PLC activity. Consistent with our earlier findings, we observed a reduction in the wing size for the knockdown of $Ca^{2+}$ signaling components. Additionally, the knockdown of PLCβ homolog

Phospholipase C at 21C *(Plc21C)* reduced the final wing size (**Fig. 3C, I**). These results imply that Gαq-mediated $Ca^{2+}$ signaling promotes growth during organ development.

In contrast, *Gαq* overexpression, which increases $Ca^{2+}$ activity in the wing disc, reduces the final wing size. As a next step, we investigated whether regulators of $Ca^{2+}$ activity contribute to the reduction in wing size. To answer this, we simultaneously overexpressed wildtype *Gαq* and downregulated $Ca^{2+}$ signaling components, such as *PLCs* and *$IP_3R$,* using RNAi. We observed that the *Gαq* overexpression, along with the knockdown of $Ca^{2+}$ signaling components, enhanced the reduction in wing size (**Fig. 3A-I**). This double perturbation analysis suggests that Gαq-mediated $Ca^{2+}$ signaling promotes growth, whereas growth inhibition due to *Gαq* overexpression occurs through a mechanism independent of $Ca^{2+}$ signaling. Altogether, our results imply that Gαq plays a dual role, where it promotes growth through a $Ca^{2+}$-dependent and inhibits growth through a $Ca^{2+}$-independent mechanism.

## Perturbation of Gαq levels resulted in increased cell density and decreased cell number

To examine whether Gαq mediates growth by regulating cell proliferation, we performed immunohistochemistry to measure Phospho-Histone H3 (PH3) levels in the wing discs. We quantified the PH3 levels in the wing disc by calculating the proliferation density. We measured the proliferation density by dividing the total area of the nuclei positive for PH3 by the pouch area (**Fig. 4**). Our analysis revealed that the cell proliferation density (PH3 per unit area of the wing disc) for both *Gαq* perturbations (overexpression or RNAi mediated inhibition) was higher than those of the control condition. Moreover, we identified that the wing discs were smaller in both *Gαq* perturbations (overexpression and downregulation) compared to the control condition (**Fig. 4D**). (**Fig. 4E**). Next, we analyzed the trichome number and trichome density, as the trichome

number indirectly represents the total number of cells in the wing. Our analysis revealed that the trichome number decreased significantly with the knockdown of *Gαq* (**Fig. 4G**), whereas *Gαq* overexpression showed no change in the trichome number. However, the trichome density was significantly higher for both overexpression and knockdown conditions (**Fig. 4I**). An increase in the trichome density (**Fig. 4I**) indicates that the average cell area is smaller for both *Gαq* perturbations. Cumulatively, these results indicate that *Gαq* overexpression reduces cell size, whereas *Gαq* knockdown reduces cell number and size.

Next, we extended the trichome analysis for individual intervein regions to investigate the effects of *Gαq* perturbations on intervein regions. Our intervein analysis showed that the trichome number decreases in all the intervein regions for the *Gαq* knockdown. In contrast, the trichome number increased for *Gαq* overexpression in the intervein regions 3, 4, and 5 (as defined in **Additional File 1, Fig. S1A**). Hedgehog (Hh) signaling has been associated with regulating the growth and patterning of the L3-L4 region of the wing, which corresponds to the intervein region 4[73]. Further, our trichome density analysis shows a different trend in the intervein regions 3 and 5. We observed that the trichome density did not show any significant difference in intervein region 5 for either inhibition of *Gαq* or overexpression of *Gαq* (**Additional File 1, Fig.S1B**). Intervein regions 3 and 5 are associated with high levels of Hedgehog (Hh) signaling and Decapentaplegic (DPP) signaling during larval development, respectively[74] (**Additional File 1, Fig.S1B** ). Together, these results confirm that perturbation to Gαq levels impacts cell proliferation and growth, thus affecting the final cell number and cell size. However, this effect is also dependent on the background signaling in different wing regions.

## Caspase-mediated apoptotic response in *Gαq* perturbations does not influence wing size

To determine whether apoptosis is stimulated by perturbing levels of *Gαq*, we performed immunostaining for death caspase-1 (*DCP-1*), a marker of programmed cell death (**Fig. 5A**). As caspases play an essential role in apoptosis[75], we quantified the area of *Dcp-1* expressing cells in both *Gαq* overexpression and knockdown conditions. Surprisingly, we discovered that either increasing or decreasing the levels of Gαq slightly decreased the Dcp-1-induced apoptotic cells in the wing disc. However, this effect was not statistically significant, given the relative background levels of Dcp-1 staining (**Fig. 5A, F**). To test whether Gαq-mediated apoptotic response determines the reduced wing size, we co-expressed both wildtype *Gαq* and baculovirus *p35* in the larval wing disc using the C765-Gal4 driver and assayed for the final adult wing phenotype. Baculovirus *p35* inhibits cell death in developing eyes and fly embryos[76] and inhibits caspases[75]. Co-expression of *Gαq*, along with p35, could not rescue the wing blade reduction. Interestingly, we observed a further reduction in the wing blade area when both *p35* and *Gαq* were expressed (*C765 > Gαq;+ > p35*) in the wing disc (**Fig. 5B-E**). In summary, inhibition of apoptosis by ectopic expression of apoptosis inhibitor *p35* did not rescue wing size reduction due to overexpression of *Gαq*. Our results thus indicate that caspase-mediated apoptotic response is not a major determinant in reducing the size of wings when *Gαq* levels are perturbed.

## *Gαq* overexpression stimulates stress response genes

To examine the transcriptional profile activated by *Gαq* overexpression, we performed RNA-seq on control discs expressing a control construct ($RyR^{RNAi,}$ which has no known effect on wings) and discs overexpressing *Gαq* (under the control of the *C765-Gal4* driver). Compared to the control discs, overexpression of *Gαq* with the C765-Gal4 driver resulted in 3613 differentially expressed genes with an adjusted p-value (p-value adjusted using Benjamini-Hochberg) of less

than 0.05 (**Additional File 1, Fig. S2A**). Of these genes, 2009 had a fold change greater than 1.5, with 878 genes upregulated and 1131 genes downregulated. To ascertain the biological processes affected by the differentially expressed genes, we performed a Gene Ontology (GO) enrichment analysis of the genes having an absolute log fold change greater than 0.6 (abs (log2FC ≥0.6)). Based on our GO analysis, we found enrichment in biological processes related to DNA replication, cuticle development, molting cycle, myofibril assembly, and protein refolding (**Additional File 1, Fig. S2B**). To investigate the biological processes that were activated or suppressed, we examined the significantly upregulated and downregulated genes separately.

First, we performed a GO enrichment analysis of the upregulated genes having a fold change greater than 1.5 (log2FC≥0.6) (**Additional File 1, Fig. S3A**). According to our GO analysis, we identified that the upregulated genes are involved in biological processes related to DNA replication, ribosome biogenesis, chromosome segregation, mitotic cell cycle process, and cuticle development. Moreover, we examined the relationships between the top enriched GO terms (**Additional File 1, Fig. S3B**) and identified that the top GO terms cluster under DNA replication, ribosome biogenesis, and cuticle development (**Additional File 1, Fig. S3B**). Additionally, we examined the genes associated with the enriched biological processes and their respective fold change values. We observed that the majority of the upregulated genes were related to the DNA replication and the mitotic cell cycle process, consistent with the possibility that the wing discs were physiologically younger and were proliferating (**Additional File 1, Fig. S3C**). Upon removing the redundant GO terms, we found that the upregulated genes are also involved in biological processes related to muscle cell development, non-membrane-bound organelle assembly, actomyosin structure organization, and protein refolding (**Additional File 1, Fig. S4**). Moreover, we found upregulation in heat shock proteins (*Hsp 70Ba*), which is related to the GO terms such as protein refolding (**Additional File 1, Fig. S4**). As well we observed an upregulation in myosin

heavy chain (*Mhc*) and myosin light chain (*Mlc2*), which are involved in the GO terms such as muscle cell development and actomyosin structure organization (**Additional File 1, Fig. S4**).

Our analysis further revealed the downregulation of Serine Protease Inhibitors (Serpin 100A, Spn 100A) (**Additional file 2**) as well as an increase in serine proteases, including multiple Jonah genes (**Additional File 1, Fig. S5**). Serine proteases are linked to the GO terms such as serine hydrolase, peptidase activity, hydrolase activity, and endopeptidase activity (**Additional File 1, Fig. S5**). Serine proteases initiate proteolysis, thus eliciting various immune responses to infection[77]. Moreover, Jonah genes are expressed during larval development and exclusively in the midgut[78]. In addition, we observed that the upregulated heat shock proteins were also associated with the hydrolase activity (**Additional File 1, Fig. S5**). Activation of heat shock proteins is a defense mechanism employed by cells in response to stress caused by the accumulation of abnormal or denatured proteins[79], [80] (proteins having defects in folding). Our GO analysis supports this result as we observe an enrichment in biological processes related to protein refolding and folding (**Additional File 1, Fig. S4**). Upregulation of heat shock proteins, particularly *Hsp70*, implies the possibility of stress accumulation in the cells. Further, induction of *Hsp70* proteins is known to reduce the growth rate in *Drosophila* cells[81, p. 70], which is potentially consistent with reduced cell size phenotypes and associated reduction in overall wing growth.

Additionally, our RNA seq analysis revealed upregulation of genes associated with chitin-based cuticle development, cuticle development, structural constituent of the cuticle, encapsulating structure, and extracellular matrix (**Additional File 1, Fig. S3-S5**). An important consideration is that the amount of cuticle proteins produced by a larva varies along with its developmental stage. Furthermore, cuticle protein synthesis depends on the 20-hydroxyecdysone (20E) levels and occurs during periods of decline in ecdysteroid levels[82]. Moreover, our analysis revealed an

increase in Dilp8 RNA levels, which also corresponds to the GO term external encapsulating structure (**Additional File 1, Fig. S5**). Dilp8 is an insulin-like peptide regulating the timing of growth and, thus, the larval-to-pupal transition[83], [84]. In summary, our analysis identified that *Gαq* overexpression increased the activity of serine proteases and heat shock proteins and affected cuticle protein synthesis. Based on our GO enrichment analysis, we conclude that the *Gαq* overexpression upregulates genes involved in DNA replication, protein folding, and cuticle protein synthesis.

As a next step, we extended our enrichment analysis to the downregulated genes (log2FC ≤ -0.6) (**Additional File 1, Fig. S6**). Enrichment analysis revealed that the significantly downregulated genes mainly correspond to biological processes such as the molting cycle, axon development, larval development, cell adhesion, and cell morphogenesis (**Additional File 1, Fig. S6A**). Upon examining the similarity between the top GO terms, we identified that locomotion, axon guidance, and cell morphogenesis were closely related (**Additional File 1, Fig. S6B**). Additionally, we examined the downregulated genes that are related to the enriched GO terms. We observed that most of the genes downregulated were involved in locomotion, taxis, neuron projection development, and biological adhesion (**Additional File 1, Fig. S6C**). We identified that the cell death genes such as *head involution defective*(*hid*) and *Dronc* were downregulated and mapped to the GO term neuron projection development. In addition, we identified downregulation in cuticular proteins (*Cuticular protein 31A*, *Cuticular protein 72Ea*, etc.) and genes related to the molting cycle (**Additional File 1, Fig. S6C**, **Fig. S7**). Moreover, our analysis revealed a strong downregulation in 20-hydroxyecdysone (20E) target genes, which include *Hormone receptor 4 (Hr4)*, *Blimp-1, and Ecdysone-induced gene 71Ee (Eig71Ee).* (**Fig. 6B&C, Additional File 1, Fig. S7C, Fig. S8**). Since ecdysone plays a pivotal role in the synthesis of cuticle proteins, we interpret that the low levels of ecdysone signaling might affect the deposition of cuticle proteins and their

timing of deposition. Collectively, these results demonstrate that *Gαq* overexpression inhibits ecdysone signaling and, as a result, affects cuticle protein synthesis.

## *Gαq* downregulation inhibits ecdysone-induced genes

To determine the transcriptomic responses affected by the *Gαq* knockdown, we performed RNA sequencing on the wing discs expressing $Gαq^{RNAi}$ and the control discs expressing $RyR^{RNAi}$. Compared to the control, 2667 genes were differentially expressed with an adjusted p-value less than 0.05. Of these genes, 1173 had absolute fold change greater than 1.5, of which 555 genes were upregulated, and 618 genes were downregulated (**Additional File 1, Fig. S9A**). To determine the biological processes enriched among the differentially expressed genes, we performed a gene ontology enrichment analysis of the genes that have a significant fold change (abs (log FC) ≥ 0.6). GO classification analysis revealed that the differentially expressed transcripts were dominant in biological processes related to transmembrane transport, cuticle development, molting cycle, and chitin-based cuticle development (**Additional File 1, Fig. S9B**). Surprisingly, the enriched GO terms for the RNAi were mostly like those observed in the *Gαq* overexpression condition. Both overexpression and downregulation of *Gαq* resulted in the enrichment of biological processes related to the cuticle proteins, axon development, and molting cycle (**Fig. 6B, Additional File 1, Fig. S9B**).

Next, we performed the Gene Ontology enrichment analysis of the significantly upregulated genes with a fold change greater than 1.5 (log FC ≥ 0.6). Our GO analysis of upregulated genes showed enrichment in biological processes related to cuticle development, mitotic spindle organization, and DNA replication (**Additional File 1, Fig. S10A**). After examining the upregulated genes relevant to the enriched GO terms, we identified that the upregulated genes were mainly involved in DNA replication and cuticle development. For instance, genes such as *Orc2* (*Origin recognition*

*complex subunit 2*), *Minichromosome maintenance 2* (*Mcm2*), and *Proliferating cell nuclear antigen* (*PCNA*) were upregulated and mapped to the GO terms such as DNA replication and DNA dependent DNA replication (**Additional File 1, Fig. S10C**). In addition, we identified upregulation in cuticle proteins such as *Cuticular protein 65Aw (Cpr65Aw*, *Cpr60D, etc.),* which are associated with the GO term cuticle development (**Additional File 1, Fig. S10C**). In addition, our analysis revealed an upregulation in serine proteases which map to the hydrolase activity and peptidase activity (**Additional File 1, Fig. S11**). Overall, our analysis of upregulated genes revealed that *Gαq* knockdown disrupted cuticle protein synthesis.

We then conducted a GO enrichment analysis of the downregulated genes to determine the biological processes associated with the downregulated genes. We identified that the downregulated genes enrich the GO terms associated with transmembrane transport, molting cycle, cell recognition, axon guidance, neuron projection guidance, and mating behavior (**Additional File 1, Fig. S12A**). After examining the gene expression relevant to the enriched GO terms, we identified that most of the downregulated genes were associated with cuticle development, molting cycle, transmembrane transport, taxis, and axon development. Interestingly, our analysis revealed downregulation in genes involved in ecdysone response regulation, including *ecdysone-induced protein 75*B (*Eig75*), which mapped to the GO terms cuticle development and molting cycle[85]. As our study revealed downregulation in genes mediating ecdysone response, we examined the gene expression related to ecdysone signaling. Interestingly, we found that the downregulated ecdysone response genes predominantly belong to the *ecdysone-induced genes 71E* family (*Eig71E*), which also are associated with the defense and immune response (**Fig.6D, Additional File 1, Fig. S13**).

*Eig71E* consists of five late-puff gene pairs that are transcribed divergently[86]. Moreover, the *Eig71E* family encodes small peptides that have biochemical characteristics similar to vertebrate

defensins and are thus assumed to provide an antimicrobial defense during metamorphosis[86]. These genes are induced by the expression of early puff genes, which are directly regulated by the steroid hormone 20-hydroxyecdysone. As the *Eig71* family belongs to late puff genes, their expression would be moderate in L3 and increase in late L3. Our data show a strong downregulation of *Eig71E* genes for $G\alpha q^{RNAi}$ compared to the control (**Additional File 1, Figure S13**). Overall, this result suggests that the wing discs expressing $G\alpha q^{RNAi}$ were physiologically less mature when compared to the control discs. Hence, we observed a downregulation in the late puff genes (**Fig. 6F**), as their expression is restricted to late larval stages. As the expression of these *Eig71E* genes is induced by ecdysone, we hypothesize that downregulation in ecdysone signaling for the discs expressing $G\alpha q^{RNAi}$ (**Fig. 6C**). Compatible with this hypothesis, we observed a downregulation in ecdysone genes such as *Hr4* and *Blimp-1* (**Fig. 6C**). The results of our study also indicated a downregulation of *Organic anion transporting polypeptide 74D* (*Oatp74D*), a solute carrier transporter that is responsible for transporting ecdysteroids into cells[87] (**Additional File 1, Fig. S12**). We further identified that the genes related to cell death were downregulated (**Additional File 1, Fig. S13**). Most genes related to cell death have a significant fold change for both overexpression and RNAi conditions (**Fig. 6A**). In summary, our study showed that the downregulation of *Gαq* in the wing disc inhibits ecdysone pathway genes **(Additional File 1, Fig. S13)**.

## Enrichment analysis of major signaling pathways

We next examined how *Gαq* perturbations affect the core signaling pathways that play imperative roles in growth and development. To achieve this, we performed an enrichment analysis to investigate the core signaling pathways that were significantly represented among the differentially expressed genes with statistically significant fold changes[88]. Our analysis identified that the Toll signaling and nuclear hormone receptor pathway were significantly enriched among the differentially expressed genes in the *Gαq* overexpression condition (**Fig.7A, B**). In the case

of *Gαq*$^{RNAi}$, the nuclear hormone receptor pathway was enriched among the differentially expressed genes. In addition, we analyzed upregulated and downregulated genes separately to identify the enrichment of core pathways among them. We found that the JAK/STAT pathway was significantly enriched among the upregulated genes for the *Gαq* overexpression, and no pathway was enriched among the upregulated genes for *Gαq*$^{RNAi}$. Next, our analysis revealed that the nuclear hormone and the Toll signaling pathway were enriched among the downregulated genes for *Gαq* overexpression. For *Gαq*$^{RNAi}$, the nuclear hormone receptor pathway was significantly enriched among the downregulated genes. In summary, our enrichment analysis revealed that the nuclear hormone receptor, JNK/STAT, and Toll pathways were significantly enriched for *Gαq* OE, whereas the nuclear hormone receptor pathway was significantly affected for *Gαq*$^{RNAi}$ (**Fig 7A, B**).

Following this, we examined gene expression changes associated with specific components of the core signaling pathways that were affected. As a first step, we examined changes in the gene expression of Toll signaling components. Toll signaling regulates cellular immune response and mediates cell elimination by regulating growth and apoptosis[89], [90]. Our analysis showed a significant upregulation in the *Toll-9* for both *Gαq* perturbations (**Additional File 2**). Additionally, we observed an approximate two-fold upregulation in *spatzle-4* (*spz4*) for *Gαq*$^{RNAi}$ and *spatzle-5* (*spz5*) for *Gαq* OE perturbations. However, we observed a downregulation in *spatzle* (*spz*) for *Gαq* OE condition (**Additional File 1, Fig. S14)**. Cleaved Spatzle is known to activate the Toll pathway in unfit cells during cell competition, thereby activating cell death[89], [91]. Upregulation of *spatzle-4* and *spatzle-5* in our analysis likely resulted from the upregulation of serine proteases. Serine proteases induce proteolytic cleavage of Spatzle during an immune response resulting in the Toll activation[92]–[94]. Cleaved Spatzle binds to the Toll receptor and initiates the nuclear localization of *Dorsal-related immunity factor* (*Dif*), resulting in the transcription of several immunity genes. Our RNA seq results showed an increase in fold change values of *Dif* for both

perturbations (**Additional File 1, Fig. S14, Fig. S15**)[95]. Of note, studies have shown that activation of Toll signaling in fat body cells inhibits insulin signaling in a non-autonomous manner, thereby resulting in reduced body growth [96]–[98]. Our analysis revealed a strong downregulation in *Phosphoinositide-dependent kinase 1* (*Pdk1*) for both *Gαq* overexpression and downregulation (**Fig. 6D, Additional File 1, Fig. S14, Fig. S15**). *Pdk1* acts upstream of *Akt* phosphorylation, and Toll signaling inhibits *Akt* phosphorylation in fat body cells[96], [98]. Normally, microbial peptides and unmethylated CpG DNA sequences activate the Toll-9 receptor. Our data shows upregulation in heat shock proteins for both *Gαq* perturbations, which can induce the activation of Toll receptors. As *Gαq* perturbations affected the expression of multiple components of Toll signaling, we propose that Gαq might play roles in Toll signaling, thus possibly affecting growth and apoptosis.

As Toll signaling activates an immune response, we asked whether immune-related genes were affected. We examined the fold change values of the immune signaling components in both *Gαq* overexpression and $Gαq^{RNAi}$ perturbations (**Additional File 1, Fig. S14, Fig. S15**). We observed a downregulation in the immune response genes for both perturbations, except for the genes including *Immune induced molecule 33* (*Im33*), *Lysozyme S* (*LysS*), and *Lysozyme B* (*LysB*). *IM33* is strongly upregulated for both perturbations and could act downstream of the Toll pathway.

Since upregulated genes in *Gαq* OE affected JAK/STAT signaling, we examined the expression change in specific components of JAK/STAT signaling. We observed that *unpaired 3* (*upd3*) was upregulated with *Gαq* overexpression with a three-fold change (**Additional File 1, Fig. S14**). *Unpaired3* (*upd3*, interleukin-6-like cytokine) is implicated in immunity, repair, gene expression, and development[99]–[101] through its activation of the JAK/STAT signaling pathway. In addition, *chinmo* (*chronologically incorrect morphogenesis),* a downstream effector of JAK/STAT signaling[102], is significantly upregulated in both $Gαq^{RNAi}$ (~12 fold) and *Gαq* OE (~46 fold)

(**Additional File 2**). Further, we identified that both perturbations increased the expression of JAK/STAT target *dilp-8* (**Fig. 6D**). The release of Dilp-8 is triggered by the activation of JAK/STAT signaling, which leads to ecdysone inhibition, thereby slowing the growth[103]. Furthermore, Dilp8 governs larval-to-pupal transition and developmental timing by regulating ecdysone signaling[84]. In summary, our study identified that *Gαq* perturbations change the expression of multiple JAK/STAT signaling components, which may contribute to either growth or apoptosis[104], [105].

As *Gαq* perturbations affected the nuclear hormone receptor pathway, we examined the fold change values of nuclear hormone receptors. Nuclear receptors bind directly to DNA and modulate gene transcription. Our data showed that the majority of the nuclear hormone receptor genes were downregulated (**Fig. 6C**), except for *fushi tarazu transcription factor 1* (*ftz-f1*) and *Ecdysone receptor* (*EcR)* (**Additional File 1, Fig. S14, Fig. S15**). Also, we observed a downregulation in ecdysone-induced genes for both perturbations. *Ftz-f1* is a nuclear receptor that transcriptionally regulates the synthesis of cuticle proteins and controls metamorophosis[82], [106]. Additionally, *EcR* is a nuclear receptor that mediates the tissue's response to ecdysteroids, which is integral to larval molting and metamorphosis[107]–[109]. *Ftz-f1* is a mid-prepupal puff gene, which also is expressed in the early second instar stage of larval development[106], [110]. In addition, *EcR* is expressed during the second half of the second instar stage of larval development[108], [110]. Thus, upregulation in *ftz-f1* and *EcR* likely resulted from the delay in larval development caused by *Gαq* perturbations. Taken together, our study indicates that perturbing Gαq levels disrupt larval development by affecting ecdysone signaling and nuclear hormone expression.

As noted above, *dilp8* expression levels were significantly upregulated. So, we asked whether this increase in *dilp8* impacts the larval to pupal transition time when *Gαq* expression levels are perturbed[103]. To determine this, we performed a developmental timing assay, wherein we recorded the larval to pupal transition time for both control and *Gαq* perturbations. Consistent with

the RNA seq finding, we observed that the larvae with *Gαq* overexpression in the wing disc cells pupariated 24 h later than the wildtype larvae (**Fig. 8A**). Similarly, we observed a delay in larval to pupal transition by 12 h for *Gαq* knockdown (**Fig. 8A**). Overall, these results imply that the disruption of Gαq levels inhibits the ecdysone signaling, therefore, delaying the development to compensate for the reduced growth. One likely interpretation of these results is that *Gαq* overexpression in the wing disc elicits immune and stress response through activation of the JAK/STAT pathway. This might activate the heat shock proteins that decrease the growth rate of the wing. JAK/STAT stimulates *dilp-8* production, which signals the brain to inhibit ecdysone synthesis, thereby slowing down development. For the $Gαq^{RNAi}$ data, we interpret that decrease in $Ca^{2+}$ activity caused by *Gαq* downregulation leads to a reduction in growth. Calcium is an important second messenger that regulates multiple cellular responses, including growth and apoptosis[26], [67], [111]. Hence, we propose that the downregulation of *Gαq* affects growth through reduced $Ca^{2+}$, thus negatively affecting ecdysone signaling. Strikingly, we observed $Ip_3R$ inhibition, along with *Gαq* overexpression, reduced the developmental delay (**Fig 8A)**. As a result, this finding supports the hypothesis that increased calcium levels are responsible for increasing the growth time that occurs through the delay in larval to pupal transition when *Gαq* is overexpressed.

## Discussion

Extracellular signals regulate organ development by embedding encoded information into the spatiotemporal dynamics of second messenger concentrations. G proteins play a vital role in mediating these external signals from GPCRs to downstream effectors by regulating key second messengers, including $Ca^{2+}$, cAMP, and $IP_3$, among others. Recent work has demonstrated that the spatiotemporal dynamics of $Ca^{2+}$ signaling correlate with changes in the final wing size in diverse ways, ranging from single-cell repetitive spiking to global traveling multicellular waves[67].

In particular, the G-protein Gαq stimulates $Ca^{2+}$ waves in developing wing discs[46]. This also is accompanied by a reduction in wing size, which correlates recurring calcium waves with growth inhibition[67]. Yet, how perturbed *Gαq* expression impacts wing size and how calcium wave production is specifically involved remain unclear.

Recently, a study reported that inhibition of GPCRs, such as *rickets (rk)*, *methuselah-like 4* (*mthl4*), *CG15744*, and *Stan,* reduce wing size[112]. Here, we confirm that the downregulation of *Gαq* in the wing disc results in smaller wings, independent of the Gal4 driver used. Additionally, we observed a similar size reduction with inhibition of *Gαq* using MS1096-Gal4 and C765-Gal4 drivers. A more severe wing expansion defect was observed in wing discs inhibiting *Gαq* driven by the nubbin-Gal4 driver. Previous work reported that three G-proteins: *Gβ13F*, *Gγ1,* and *Gαs,* are essential for proper wing expansion[113]. Here, our study identified that *Gαq* expression levels also could impact wing expansion. A recent study by Sobala et al. reported that *Gαs*, *Gαq*, and *Gβ13F* are expressed at different stages in the pupal wing disc during pupal wing development[114]. Our study confirms this observation as *Gαq* downregulation leads to defects in pupal wing expansion. Saad et al. reported similar post-expansion defects when GPCRs such as the *methuselah* (*mth*)-like family receptors *mthl6*, *mthl8* and *mthl9* were downregulated in the *Drosophila* wing under nubbin gal4 driver[112]. Future studies are required to identify the GPCRs that function upstream of Gαq to regulate organ growth or expansion phenotypes.

This study highlights the importance of Gαq homeostasis during organ growth. Gαq stimulates $IP_3$ production, which activates the $IP_3R$ channel to release $Ca^{2+}$ from ER[19], [115]–[120]. Our previous experimental studies investigated the emergence of diverse classes of spatiotemporal $Ca^{2+}$ dynamics in both *ex vivo* cultures and *in vivo*[46], [67]. Here, our *in vivo* imaging studies revealed an increase in $Ca^{2+}$ activity and strong intercellular calcium wave (ICW) formation with *Gαq* overexpression (**Fig. 1B**), consistent with past *ex vivo*. This result confirms that Gαq

stimulates $Ca^{2+}$ release from ER into the cytoplasm through the activation of its downstream effectors. Our previous studies show that normal physiological levels of calcium signaling promote wing disc growth[67]. Interestingly, further elevating calcium signaling through *Gαq* overexpression reduces wing size, thereby suggesting additional Gαq downstream effectors participating in growth regulation.

To assess whether Gαq-mediated $Ca^{2+}$ signaling impacts the size phenotype, we performed genetic interaction experiments by overexpressing *Gαq* and co-expressing RNAi constructs targeting downstream regulators of $Ca^{2+}$ signaling. Surprisingly, we found a statistically significant enhancement in wing size reduction when $Ca^{2+}$ signaling components were inhibited along with *Gαq* overexpression. Thus, we hypothesize that the primary growth-inhibiting activity of Gαq may be through a mechanism independent of $Ca^{2+}$ activity. Moreover, our trichome analysis for *Gαq* overexpression shows that the intervein regions associated with Hh signaling show a different trend in trichome number and density when compared to the overall wing. Our findings from this study imply that Gαq interacts with other growth signaling pathways, thus negatively influencing growth. Together, these results demonstrate the dual action performed by Gαq during wing development, where it stimulates growth through downstream $IP_3R/Ca^{2+}$ activity and inhibits growth through its interactions with mitogenic pathways independent of $Ca^{2+}$ activity. In addition to *Gαq*, our results show that the depletion of Plc21c levels, which is homologous to mammalian PLCβ, results in decreased adult wing size. This further supports our findings that the depletion of $Ca^{2+}$ signaling components leads to a reduction in wing growth[67]. Future studies are required to investigate the role of Gαq mediated PKC activity in regulating the growth independent of the $Ca^{2+}$ signaling.

Our molecular and transcriptomic analysis investigated the downstream signaling motifs affected in response to *Gαq* perturbations. Our PH3 studies showed an increase in proliferation density

for both overexpression and RNAi wing discs. The higher proliferation density observed may be due to wing discs being physiologically younger than the control discs, so they proliferate more rapidly. Our transcriptomic study further confirms this result as we observed an upregulation in genes related to DNA replication for both *Gαq* perturbations. However, the trichome number studies showed a reduction in the overall trichome number for $Gαq^{RNAi}$, whereas it did not show any significant change for *Gαq* overexpression. Moreover, the trichome density increased for both perturbations compared to the control and can be attributed to the reduced wing size. As cell size and number are indirect readouts of growth and proliferation, this result establishes that Gαq homeostasis is necessary for maintaining an optimal growth rate and duration of organ growth. Several studies identify the active role of Gαq while promoting growth and proliferation in different systems[14], [15], [121]. For example, Gαq mediates the PI3K activation and the subsequent airway smooth muscle growth[122]. In addition, GPCRs stimulate YAP phosphorylation via Gαq[123], thus regulating Hippo signaling in HEK cells. Taken together, our results demonstrate that Gαq impacts the final wing size by tuning growth and proliferation.

Further, inhibition and overexpression of *Gαq* in the wing disc slightly decrease the total number of cells undergoing apoptosis. Furthermore, our RNA-seq analysis shows both upregulation and downregulation of apoptotic genes for both overexpression and RNAi conditions (**Fig. 6A**). Studies have shown that Gαq regulates cell death both positively and negatively in multiple systems[111], [124], [125]. For example, *Gαq* expression decreases apoptosis in cardiomyocytes through EGFR activation[124]. In addition, Gαq mediated ICWs inhibit excessive apoptosis during epithelial wound healing[126]. Conversely, Gαq activation by GPCR induces apoptosis by reducing PKC-dependent AKT activity in prostate cancer cells[125]. Collectively, these studies provide evidence that Gαq either stimulates or inhibits apoptosis. Consistent with these studies, our transcriptomic study shows that *Gαq* perturbations resulted in dysregulation of the apoptotic genes. However, our results show that inhibition of apoptosis along with *Gαq* overexpression

686 could not rescue the wing size phenotype, thereby suggesting a minimal role of apoptosis in
687 regulating Gαq-mediated growth reduction.
688
689 Our transcriptomic study revealed that *Gαq* overexpression activates stress response genes,
690 which include heat shock proteins and serine proteases. The expression of serine proteases is
691 increased as serpins, which inhibit serine proteases, were downregulated in our RNA-seq data.
692 In addition, our findings show that JNK components, including *dilp8*, *upd3,* and *chinmo* were
693 significantly upregulated. JNK signaling induces stress and immune response[127]–[130] and
694 initiates compensatory proliferation[130]. Importantly, JNK signaling induces *dilp8* expression in
695 the wing disc in response to tissue damage or stress[83]. Further, increased Dilp8 levels
696 communicate with the brain to inhibit the ecdysone synthesis, thereby slowing growth[83], [131].
697 Consistent with these reports, we found that *Gαq* overexpression decreased the expression of
698 20E-dependent genes. Moreover, our developmental assay confirms this result as we observed
699 a delay in larval to pupal transition for flies expressing *Gαq* in the wing disc. This developmental
700 delay is strikingly similar to that observed when *dilp-8* is overexpressed in the wing disc[83], [84].
701 Studies have shown that different *Gα* subtypes such as *Gαo, $G\alpha_{16}$* induce mitogenic activity
702 through activation of JAK/STAT signaling[38], [132], [133]. For instance, the constitutively active
703 form of *Gαo* induces activation of STAT3 in NIH-3T3 cells and subsequent cell
704 transformation[133, p. 3]. In addition, Heasley et al. have shown that expression of the
705 constitutively active form of *$G\alpha_{16}$* inhibits growth and activates JNK signaling in small lung
706 carcinoma cell lines (SLC)[39]. By contrast, sustained activation of Gαq signaling induces cell
707 death in GABAergic medium spiny neurons via activation of JNK signaling[134]. These studies
708 indicate the active role of JAK/STAT signaling in Gαq mediated growth and apoptosis.
709 Cumulatively, our results demonstrate that *Gαq* overexpression regulates JNK signaling genes,
710 which might possibly regulate apoptosis and proliferation, thereby affecting the final wing size.
711 While many studies have investigated the mechanisms underlying the transmission of proliferative

712 signals through GPCR stimulation *in vitro*, further research is required to elucidate how G proteins
713 encode mitogenic signals *in vivo*[14], [135].
714
715 Next, our RNA seq analysis of *Gαq*$^{RNAi}$ indicates that the nuclear hormone receptor-related genes
716 were affected (**Fig. 6E & 7B**). Our analysis indicated that DNA replication was enriched among
717 the upregulated genes. Moreover, the downregulated genes were primarily involved in biological
718 processes related to cuticle development, molting cycle, taxis, and transmembrane transport.
719 Interestingly, we observed downregulation in genes mediating ecdysone response (**Fig. 6E**),
720 thereby resulting in the downregulation of ecdysone-induced genes (**Additional File 1, Fig. S13**
721 **and Fig. S15**). Specifically, the *Ecdysone-induced genes 71E* family (*Eig71E*), which are
722 regulated by Ecdysone-induced primary response genes, were downregulated (**Additional File**
723 **1, Fig. S13, Additional File 3)**. A further finding was an increase in Dilp-8 levels, which may
724 explain the inhibition of genes related to ecdysone signaling. Our developmental assay further
725 confirmed this as we observed an approximate twelve-hour delay in the pupariation of flies
726 expressing *Gαq*$^{RNAi}$. Interestingly, we identified a similar trend in gene expression profile for both
727 *Gαq*$^{RNAi}$ and *Gαq* overexpression conditions. However, the extent of gene activation or
728 suppression is statistically less in *Gαq*$^{RNAi}$ when compared to the *Gαq* overexpression. These
729 results suggest a common compensatory mechanism in a cell operating in response to
730 dysregulation of Gαq homeostasis. Moreover, our trichome analysis of *Gαq*$^{RNAi}$ showed a
731 reduction in the cell number, thereby indicating that the reduction in the wing disc growth is caused
732 by the lack of calcium signaling. Collectively, our RNA seq results demonstrated that disruption
733 to Gαq homeostasis reduced growth and increased developmental time. Further, the increased
734 developmental time caused by *Gαq* overexpression occurs through $Ca^{2+}$ activity. Significantly, we
735 observed that inhibition of $Ca^{2+}$ signaling through $Ip_3R$ knockdown rescues the development delay
736 caused by *Gαq* overexpression. However, the knockdown of $Ip_3R$ along with *Gαq* overexpression

737 reduced wing size, thereby implying that $Ca^{2+}$ signaling promotes proliferation in the wing disc by
738 regulating the developmental time.
739
740 Importantly, our RNA seq data revealed a reduction in the expression of serine protease inhibitors,
741 thus resulting in an increase in the expression of serine proteases, including Jonah genes, which
742 are key proteolytic enzymes (**Additional File 2)**. Moreover, serine protease cascades are known
743 to elicit immune responses by inducing proteolytic cleavage of *spz*[92]. Our enrichment analysis
744 investigating the core signaling pathways indicated that the nuclear hormone receptor, Toll
745 signaling, and JAK/STAT were significantly affected in the *Gαq* overexpression condition. This
746 result confirms that disruption to Gαq homeostasis parallels signals related to tissue damage
747 response, thereby eliciting stress and immune response. Several studies have reported the role
748 of G proteins in mediating immune response and autoimmunity[136]–[138]. For example, Zhu. et
749 al. reported that XLG2, a functional *Gα* protein, positively regulates immune response to provide
750 disease resistance in plants[139]. Interestingly, studies have shown that the activation of immune
751 signaling occurs at the expense of growth[89]. Further investigations are needed to explore the
752 crosstalk mechanisms between Gαq and immune regulation during organ growth.
753
754 Of note, our transcriptomic analysis of *Gαq* OE shows a strong upregulation in the orphan GPCR
755 Methuselah-like 8 (mthl8) with a striking log2 fold change of 11.5 (**Additional File 4**). *Mthl-8* has
756 been shown to impact wing expansion[140]. In addition, the family of Methuselah genes is known
757 to be involved in longevity and stress resistance[141]. Recent work in Lepidoptera suggests that
758 GPCRs with homology to the Methuselah family of receptors may play important, unresolved roles
759 in mediating the key hormone ecdysone[63], [142]. Importantly, it has been shown that *mthl-8* is
760 a potential target of the JNK signaling in the *Drosophila* eye disc[143]. Collectively, our results
761 imply a crosstalk between Gαq and GPCRs such as mthl-8. Further investigations are needed to
762 elucidate the role of G proteins in regulating the expression of signal transducers such as GPCRs.

763 Moreover, studies are needed to clarify the subcellular location and functional activity of Gαq and
764 related GPCRs. Recently, GPCRs have been found to be active not only in the outer cell
765 membrane but associated with the inner membranes of organelles within the cell[144], [145]. Also,
766 further investigation is needed to map out key molecular players activating Gαq-mediated ICWs
767 *in vivo*. For instance, recent studies have indicated that growth-blocking peptide (Gbps) binds to
768 Mthl10 receptors and triggers Gαq mediated ICWs in the *Drosophila* wing disc[48]. Understanding
769 the growth regulatory mechanisms acting through G-proteins may lead to broadly applicable
770 insights into cancer therapeutics and drug development[141], [146].

771

772 ## Conclusions

773 In summary, our study has decoded the downstream impacts of perturbing *Gαq* expression. Gαq
774 activity is sufficient to stimulate intercellular calcium waves and is a key regulator of $Ca^{2+}$ activity
775 during development and wound healing. Our study characterized the multiple growth modules
776 impacted by *Gαq* perturbations and their roles in facilitating organ growth control during
777 development. An intriguing finding is that there exist similar changes in gene expression for
778 $Gαq^{RNAi}$ and *Gαq* OE conditions, which suggests that homeostasis of *Gαq* expression is
779 necessary for proper growth and development. Overall, our findings from this work suggest that
780 a central functional role of Gαq-mediated $Ca^{2+}$ signaling is to coordinate the growth status of
781 peripheral organs to the brain by upregulating Dilp8, thereby mediating the “crosstalk” between
782 developing organs and “the control center” of the brain (**Fig. 6E**). Thus, tissue wide $Ca^{2+}$ waves
783 generated by Gαq activity coordinates the response to wounding or other stressors to extend the
784 developmental time and reduce growth.

785

## Materials and methods

### Fly stocks

*Drosophila* stocks were grown on standard laboratory cornmeal food. All crosses were set up at 25°C. The following stocks were used for the experiment: C765-Gal4 y[1] w[*]; P{w[+mW.hs]=GawB}C-765 (BDSC:36523), nubbin-GAL4, UAS-Dcr-2 (BDSC:25754), MS1096-GAL4, UAS-Dcr-2 (BDSC:25706), UAS-Gαq (BDSC:30734), UAS-Galpha49B RNAi (BDSC:36775), w; Sco/CyO; Dr/TM6B, Tb (gift of Carthew Lab), w; Sco/CyO; MKRS/TM6B, Tb (gift from Carthew lab), w; UAS-Gαq/CyO; C765-Gal4/TM6B,Tb (generated in this study), w; UAS-Gαq,C765-Gal4/Cyo-TM6B,Tb (generated in this study), UAS-Itpr RNAi (BDSC:25937), UAS-p35 ( BDSC #6298), UAS-Plc21C RNAi (BDSC: 33719), UAS-sl RNAi (BDSC:32906), UAS-Rya-r44F RNAi (BDSC:31540), nub-GAL4, UAS-GCaMP6f/CyO (recombinant line made in Zartman Lab).

### Immunohistochemistry and imaging of fixed samples

The imaginal wing discs were dissected in Phosphate Buffered Saline (PBS) (#P5368, Millipore-Sigma). Following the dissection of the wing discs, they were fixed in 4% PFA for 20 minutes at room temperature, followed by three 10-minute washes in PBT (0.03% Triton X-100 (#T9284, Sigma-Aldrich) in PBS). Next, discs were blocked in 5% Normal Goat Serum (NGS) (#NC9660079; Jackson Immuno Research Laboratories, West Grove, PA) for 30 minutes and followed by overnight incubation with primary antibodies at 4°C. The following primary antibodies were used: PH3 (#9701S, Cell Signaling), diluted to 1:800 in 5% NGS, and DCP-1 (#9578S; Cell Signaling), diluted to 1:100 in 5% NGS. Incubation of the primary antibodies was followed by three 15-minute washes with PBT and subsequent incubation with Alexa Fluor-conjugated secondary antibodies (1:500 in 5%NGS) and DAPI (# D9542; Millipore Sigma) (1:1000) for 2-3 hours at room temperature in the dark. After this, wing discs were washed with PBT overnight at 4°C, followed

by two 15-minute washes at room temperature. Discs were next mounted in Vectashield (# H-1000, Vector Laboratories) on a 24x66 mm coverslip and covered by a 22x22 coverslip, and sealed with clear nail polish by the sides. Images of mounted wing discs were obtained using a Nikon Eclipse Ti confocal microscope with a Yokogawa spinning disk (Tokyo, Japan) at a magnification of 40x (oil objective, NA 1.30).

## In vivo imaging setup

Third instar wandering larvae were collected and rinsed in deionized water prior to imaging. A coverslip was used to image the larvae after they had been dried and adhered to a cover with Scotch tape. The larvae were attached with their spiracles facing the coverslip to align the wing discs toward the microscope. An EVOS FL Auto microscope was used to image the larvae at a magnification of 20x for 20 minutes. The images were taken every 15 seconds.

## RNA extraction

RNA was isolated using RNeasy Mini Kit (#74104; QIAGEN), using a standard procedure with DNase on column digestion (RNase-free DNase set. #79254, QIAGEN). RNA was eluted in RNase DNase-free water provided by the RNeasy Mini Kit. Samples from multiple days of dissection were pooled such that each biological replica would have 79 WDs. To assess the RNA quantity and quality, we performed QC using Qubit and Agilent Bioanalyzer and polled samples from multiple days of RNA isolation to achieve at least 50ng of RNA per sample or higher.

## Sequencing

RNASeq libraries were prepared and sequenced across one lane of an Illumina NextSeq v2.5 (Mid Output 150 cycle) flow cell. Each library was prepared using the NEBNext Ultra II Directional

RNA. Library Prep kit and the NEB mRNA Magnetic Isolation Module. We performed QC and quantitation on the library pool using the Qubit dsDNA Agilent Bioanalyzer DNA. High Sensitivity Chip, and Kapa Illumina Library Quantification qPCR assays. The sequencing form was paired-end 75bp. Base calling was done by Illumina Real Time Analysis (RTA) v2 software.

## Processing of sequencing data

We trimmed the raw sequences of adapters with Trimmomatic version 0.39[147] and assessed for quality with FastQC v 0.11.8[148]. Trimmed sequences were aligned to the *Drosophila* genome, and Ensembl built *Drosophila melanogaster.*BDGP6.32.104.gtf, Berkeley *Drosophila* Genome Project (BDGP, Release 6, Aug. 2014), using Dmel_Release_6.01 version annotations and HISAT2 version 2.1.0[149]. SAMtools version 1.9 was used to sort the corresponding alignments[150]. Read counts were generated with HTSeq-count version 0.11.2[151]. Subsequent statistics were completed in R (R Core Team, 2014), implementing the edgeR library version 3.36.0[152]–[155]. Using the Ensembl version of BioMart, Gene names and GO terms were identified[156].

## Quantification of adult wings and statistics

Using ImageJ, we measured the total area of the wings. The wing margin was traced by following veins L1 and L5, and the hinge region was excluded from the size analysis. All statistical analyses were performed using R and Excel. Student t-tests were performed to assess the statistical significance of our comparisons. P-value, standard deviation, and sample size (n) are provided in each figure and legend.

## Developmental timing assay

Virgins were 1-3 days old when mated with males. Crosses were mated 24 h prior and transferred to a vial for egg collection. Fertilized eggs from each cross were collected for eight hours in a fresh vial with corn meal food and then transferred to a new vial. After egg laying, pupae were manually scored in 12-hour intervals for ten days. For C765>Gαq + >$RyR^{RNAi}$ and C765>Gαq + >$Ip_3R^{RNAi}$, pupae were manually counted in 24-hour intervals for approximately 6 to 7 days.

## Acknowledgments

The work in this paper was supported by NIH Grant R35GM124935, NSF Award CBET-1553826, and EMBRIO Institute, contract #2120200, a National Science Foundation (NSF) Biology Integration Institute. Notre Dame Genomics & Bioinformatics Core Facility provided services related to RNA sequencing. The authors would also like to thank members of the Zartman lab for helpful discussions. We would like to thank Giorgia Giordano for her help in the project.

## Author contributions

VVK performed experiments, analyzed data, and wrote the paper. DKS conceived the study, performed experiments, analyzed data, and wrote the paper. MU performed experiments, analyzed data, and wrote the paper. DG and NK performed experiments and analyzed data. JL performed the RNA seq analysis. JJZ conceived the study, analyzed data, wrote the paper, and supervised the study.

## Data Availability

Differential gene expression analysis data obtained from our RNA sequencing study is available in Additional File 3 and Additional File 4. The RNA sequencing raw data and the

wing image data obtained during the current study is available from the corresponding author on reasonable request.

**Conflict of interests**

The authors declare no conflicts of interest.

## References

[1] I. K. Hariharan, “Organ Size Control: Lessons from Drosophila,” *Developmental Cell*, vol. 34, no. 3, pp. 255–265, Aug. 2015, doi: 10.1016/j.devcel.2015.07.012.

[2] E. Hafen and H. Stocker, “How Are the Sizes of Cells, Organs, and Bodies Controlled?,” *PLoS Biol*, vol. 1, no. 3, p. e86, Dec. 2003, doi: 10.1371/journal.pbio.0000086.

[3] I. Conlon and M. Raff, “Size Control in Animal Development,” *Cell*, vol. 96, no. 2, pp. 235–244, Jan. 1999, doi: 10.1016/S0092-8674(00)80563-2.

[4] R. M. Neto-Silva, B. S. Wells, and L. A. Johnston, “Mechanisms of growth and homeostasis in the Drosophila wing,” *Annu Rev Cell Dev Biol*, vol. 25, pp. 197–220, 2009, doi: 10.1146/annurev.cellbio.24.110707.175242.

[5] N. Arora *et al.*, “A process engineering approach to increase organoid yield,” *Development*, p. dev.142919, Jan. 2017, doi: 10.1242/dev.142919.

[6] P. J. Bryant and P. Simpson, “Intrinsic and Extrinsic Control of Growth in Developing Organs,” *The Quarterly Review of Biology*, vol. 59, no. 4, pp. 387–415, Dec. 1984, doi: 10.1086/414040.

[7] A. Roselló-Díez and A. L. Joyner, “Regulation of Long Bone Growth in Vertebrates; It Is Time to Catch Up,” *Endocrine Reviews*, vol. 36, no. 6, pp. 646–680, Dec. 2015, doi: 10.1210/er.2015-1048.

[8] R. Lappano and M. Maggiolini, “GPCRs and cancer,” *Acta Pharmacol Sin*, vol. 33, no. 3, Art. no. 3, Mar. 2012, doi: 10.1038/aps.2011.183.

[9] A. G. Gilman, “G Proteins: Transducers of Receptor-Generated Signals,” *Annual Review of Biochemistry*, vol. 56, no. 1, pp. 615–649, 1987, doi: 10.1146/annurev.bi.56.070187.003151.

[10] M. I. Simon, M. P. Strathmann, and N. Gautam, “Diversity of G Proteins in Signal Transduction,” *Science*, vol. 252, no. 5007, pp. 802–808, May 1991, doi: 10.1126/science.1902986.

[11] J. R. Hepler and A. G. Gilman, “G proteins,” *Trends in Biochemical Sciences*, vol. 17, no. 10, pp. 383–387, Oct. 1992, doi: 10.1016/0968-0004(92)90005-T.

[12] V. Radhika and N. Dhanasekaran, “Transforming G proteins,” *Oncogene*, vol. 20, no. 13, pp. 1607–1614, Mar. 2001, doi: 10.1038/sj.onc.1204274.

[13] T. Imamura *et al.*, “G Alpha-q/11 Protein Plays a Key Role in Insulin-Induced Glucose Transport in 3T3-L1 Adipocytes,” *Molecular and Cellular Biology*, vol. 19, no. 10, pp. 6765–6774, Oct. 1999, doi: 10.1128/MCB.19.10.6765.

[14] K. B. Hubbard and J. R. Hepler, “Cell signalling diversity of the Gqα family of heterotrimeric G proteins,” *Cellular Signalling*, vol. 18, no. 2, pp. 135–150, Feb. 2006, doi: 10.1016/j.cellsig.2005.08.004.

[15] N. Dhanasekaran, S.-T. Tsim, J. M. Dermott, and D. Onesime, “Regulation of cell proliferation by G proteins,” *Oncogene*, vol. 17, no. 11, Art. no. 11, Sep. 1998, doi: 10.1038/sj.onc.1202242.

[16] C. C. Malbon, “G proteins in development,” *Nat Rev Mol Cell Biol*, vol. 6, no. 9, Art. no. 9, Sep. 2005, doi: 10.1038/nrm1716.

[17] S. G. F. Rasmussen *et al.*, “Crystal structure of the β2 adrenergic receptor–Gs protein complex,” *Nature*, vol. 477, no. 7366, Art. no. 7366, Sep. 2011, doi: 10.1038/nature10361.

[18] T. M. Wilkie, P. A. Scherle, M. P. Strathmann, V. Z. Slepak, and M. I. Simon, “Characterization of G-protein alpha subunits in the Gq class: expression in murine tissues and in stromal and hematopoietic cell lines.,” *Proceedings of the National Academy of Sciences*, vol. 88, no. 22, pp. 10049–10053, Nov. 1991, doi: 10.1073/pnas.88.22.10049.

[19] S. G. Rhee, “Regulation of Phosphoinositide-Specific Phospholipase C,” *Annual Review of Biochemistry*, vol. 70, no. 1, pp. 281–312, 2001, doi: 10.1146/annurev.biochem.70.1.281.

[20] U. Kikkawa, A. Kishimoto, and Y. Nishizuka, “The Protein Kinase C Family: Heterogeneity and Its Implications,” *Annual Review of Biochemistry*, vol. 58, no. 1, pp. 31–44, 1989, doi: 10.1146/annurev.bi.58.070189.000335.

[21] L. Jackson, A. Qifti, K. M. Pearce, and S. Scarlata, “Regulation of bifunctional proteins in cells: Lessons from the phospholipase Cβ/G protein pathway,” *Protein Science*, vol. 29, no. 6, pp. 1258–1268, 2020, doi: 10.1002/pro.3809.

[22] D. Kamato *et al.*, “Structure, Function, Pharmacology, and Therapeutic Potential of the G Protein, Gα/q,11,” *Frontiers in Cardiovascular Medicine*, vol. 2, 2015, Accessed: Aug. 24, 2022. [Online]. Available: https://www.frontiersin.org/articles/10.3389/fcvm.2015.00014

[23] W. D. Singer, H. A. Brown, and P. C. Sternweis, “Regulation of Eukaryotic Phosphatidylinositol-Specific Phospholipase C and Phospholipase D,” *Annual Review of Biochemistry*, vol. 66, no. 1, pp. 475–509, 1997, doi: 10.1146/annurev.biochem.66.1.475.

[24] T. K. Harden, G. L. Waldo, S. N. Hicks, and J. Sondek, “Mechanism of Activation and Inactivation of Gq/Phospholipase C-β Signaling Nodes,” *Chem. Rev.*, vol. 111, no. 10, pp. 6120–6129, Oct. 2011, doi: 10.1021/cr200209p.

[25] P. A. Brodskiy *et al.*, “Decoding Calcium Signaling Dynamics during Drosophila Wing Disc Development,” *Biophysical Journal*, vol. 116, no. 4, Art. no. 4, Feb. 2019, doi: 10.1016/j.bpj.2019.01.007.

[26] P. A. Brodskiy and J. J. Zartman, “Calcium as a signal integrator in developing epithelial tissues,” *Physical biology*, vol. 15, no. 5, Art. no. 5, 2018.

[27] P. A. Galvin-Parton, X. Chen, C. M. Moxham, and C. C. Malbon, “Induction of Gαq-specific Antisense RNA in Vivo Causes Increased Body Mass and Hyperadiposity *,” *Journal of Biological Chemistry*, vol. 272, no. 7, pp. 4335–4341, Feb. 1997, doi: 10.1074/jbc.272.7.4335.

[28] J. Baumbach, Y. Xu, P. Hehlert, and R. P. Kühnlein, “Gαq, Gγ1 and Plc21C control Drosophila body fat storage,” *Journal of Genetics and Genomics*, vol. 41, no. 5, Art. no. 5, 2014.

[29] S. Offermanns, L.-P. Zhao, A. Gohla, I. Sarosi, M. I. Simon, and T. M. Wilkie, “Embryonic cardiomyocyte hypoplasia and craniofacial defects in Gαq. Gα11-mutant mice,” *The EMBO Journal*, vol. 17, no. 15, pp. 4304–4312, Aug. 1998, doi: 10.1093/emboj/17.15.4304.

[30] S. Offermanns *et al.*, “Impaired motor coordination and persistent multiple climbing fiber innervation of cerebellar Purkinje cells in mice lacking Galphaq,” *Proc Natl Acad Sci U S A*, vol. 94, no. 25, pp. 14089–14094, Dec. 1997, doi: 10.1073/pnas.94.25.14089.

[31] “Loss of Gq/11 family G proteins in the nervous system causes pituitary somatotroph hypoplasia and dwarfism in mice,” 2005.

[32] C. D. Van Raamsdonk, K. R. Fitch, H. Fuchs, M. H. de Angelis, and G. S. Barsh, “Effects of G-protein mutations on skin color,” *Nat Genet*, vol. 36, no. 9, Art. no. 9, Sep. 2004, doi: 10.1038/ng1412.

[33] M. D. Vivo, J. Chen, J. Codina, and R. Iyengar, “Enhanced phospholipase C stimulation and transformation in NIH-3T3 cells expressing Q209LGq-alpha-subunits.,” *Journal of Biological Chemistry*, vol. 267, no. 26, pp. 18263–18266, Sep. 1992, doi: 10.1016/S0021-9258(19)36952-2.

[34] M. De Vivo and R. Iyengar, “Activated Gq-alpha potentiates platelet-derived growth factor-stimulated mitogenesis in confluent cell cultures.,” *Journal of Biological Chemistry*, vol. 269, no. 31, pp. 19671–19674, Aug. 1994, doi: 10.1016/S0021-9258(17)32070-7.

[35] H. Zeng, D. Zhao, S. Yang, K. Datta, and D. Mukhopadhyay, “Heterotrimeric Gαq/Gα11 Proteins Function Upstream of Vascular Endothelial Growth Factor (VEGF) Receptor-2 (KDR) Phosphorylation in Vascular Permeability Factor/VEGF Signaling*,” *Journal of*

*Biological Chemistry*, vol. 278, no. 23, pp. 20738–20745, Jun. 2003, doi: 10.1074/jbc.M209712200.

[36] R. D. Peavy, M. S. S. Chang, E. Sanders-Bush, and P. J. Conn, "Metabotropic Glutamate Receptor 5-Induced Phosphorylation of Extracellular Signal-Regulated Kinase in Astrocytes Depends on Transactivation of the Epidermal Growth Factor Receptor," *J. Neurosci.*, vol. 21, no. 24, pp. 9619–9628, Dec. 2001, doi: 10.1523/JNEUROSCI.21-24-09619.2001.

[37] J. Yamauchi, M. Nagao, Y. Kaziro, and H. Itoh, "Activation of p38 Mitogen-activated Protein Kinase by Signaling through G Protein-coupled Receptors: INVOLVEMENT OF Gβγ AND Gαq/11 SUBUNITS*," *Journal of Biological Chemistry*, vol. 272, no. 44, pp. 27771–27777, Oct. 1997, doi: 10.1074/jbc.272.44.27771.

[38] R. K. H. Lo, H. Cheung, and Y. H. Wong, "Constitutively Active Gα16 Stimulates STAT3 via a c-Src/JAK- and ERK-dependent Mechanism*," *Journal of Biological Chemistry*, vol. 278, no. 52, pp. 52154–52165, Dec. 2003, doi: 10.1074/jbc.M307299200.

[39] L. E. Heasley *et al.*, "Discordant Signal Transduction and Growth Inhibition of Small Cell Lung Carcinomas Induced by Expression of GTPase-deficient Gα16(∗)," *Journal of Biological Chemistry*, vol. 271, no. 1, pp. 349–354, Jan. 1996, doi: 10.1074/jbc.271.1.349.

[40] C. García-Hoz, G. Sánchez-Fernández, M. T. Díaz-Meco, J. Moscat, F. Mayor, and C. Ribas, "Gαq Acts as an Adaptor Protein in Protein Kinase Cζ (PKCζ)-mediated ERK5 Activation by G Protein-coupled Receptors (GPCR)♦," *J Biol Chem*, vol. 285, no. 18, pp. 13480–13489, Apr. 2010, doi: 10.1074/jbc.M109.098699.

[41] C. D. Van Raamsdonk *et al.*, "Frequent somatic mutations of GNAQ in uveal melanoma and blue naevi," *Nature*, vol. 457, no. 7229, Art. no. 7229, Jan. 2009, doi: 10.1038/nature07586.

[42] C. D. Van Raamsdonk *et al.*, "Mutations in GNA11 in Uveal Melanoma," *New England Journal of Medicine*, vol. 363, no. 23, pp. 2191–2199, Dec. 2010, doi: 10.1056/NEJMoa1000584.

[43] G. Kalinec, A. J. Nazarali, S. Hermouet, N. Xu, and J. S. Gutkind, "Mutated alpha subunit of the Gq protein induces malignant transformation in NIH 3T3 cells," *Molecular and Cellular Biology*, vol. 12, no. 10, pp. 4687–4693, Oct. 1992, doi: 10.1128/mcb.12.10.4687-4693.1992.

[44] N. X. Qian, M. Russell, A. M. Buhl, and G. L. Johnson, "Expression of GTPase-deficient G alpha 16 inhibits Swiss 3T3 cell growth," *Journal of Biological Chemistry*, vol. 269, no. 26, pp. 17417–17423, Jul. 1994, doi: 10.1016/S0021-9258(17)32455-9.

[45] N.-X. Qian, S. Winitz, and G. L. Johnson, "Epitope-tagged Gq a subunits: Expression of GTPase-deficient a subunits persistently stimulates phosphatidylinositol-specific phospholipase C but not mitogen-activated protein kinase activity regulated by the M1 muscarinic acetylcholine receptor," *Proc. Natl. Acad. Sci. USA*, p. 5, 1993.

[46] D. K. Soundarrajan, F. J. Huizar, R. Paravitorghabeh, T. Robinett, and J. J. Zartman, "From spikes to intercellular waves: Tuning intercellular calcium signaling dynamics modulates organ size control," *PLOS Computational Biology*, vol. 17, no. 11, p. e1009543, Nov. 2021, doi: 10.1371/journal.pcbi.1009543.

[47] E. K. Shannon *et al.*, "Multiple Mechanisms Drive Calcium Signal Dynamics around Laser-Induced Epithelial Wounds," *Biophysical Journal*, vol. 113, no. 7, pp. 1623–1635, Oct. 2017, doi: 10.1016/j.bpj.2017.07.022.

[48] J. T. O'Connor *et al.*, "Proteolytic activation of Growth-blocking peptides triggers calcium responses through the GPCR Mthl10 during epithelial wound detection," *Developmental Cell*, vol. 56, no. 15, pp. 2160-2175.e5, Aug. 2021, doi: 10.1016/j.devcel.2021.06.020.

[49] A. Buchmann, M. Alber, and J. J. Zartman, “Sizing it up: the mechanical feedback hypothesis of organ growth regulation,” *Semin Cell Dev Biol*, vol. 35, pp. 73–81, Nov. 2014, doi: 10.1016/j.semcdb.2014.06.018.

[50] M. C. Diaz de la Loza and B. J. Thompson, “Forces shaping the Drosophila wing,” *Mech Dev*, vol. 144, no. Pt A, pp. 23–32, Apr. 2017, doi: 10.1016/j.mod.2016.10.003.

[51] T. Chorna and G. Hasan, “The genetics of calcium signaling in Drosophila melanogaster,” *Biochim Biophys Acta*, vol. 1820, no. 8, pp. 1269–1282, Aug. 2012, doi: 10.1016/j.bbagen.2011.11.002.

[52] B. K. Tripathi and K. D. Irvine, “The wing imaginal disc,” *Genetics*, p. iyac020, Feb. 2022, doi: 10.1093/genetics/iyac020.

[53] J. B. Duffy, “GAL4 system in Drosophila: a fly geneticist’s Swiss army knife,” *Genesis*, vol. 34, no. 1–2, pp. 1–15, Oct. 2002, doi: 10.1002/gene.10150.

[54] E. N. Howe *et al.*, “Rab11b-mediated integrin recycling promotes brain metastatic adaptation and outgrowth,” *Nat Commun*, vol. 11, no. 1, Art. no. 1, Jun. 2020, doi: 10.1038/s41467-020-16832-2.

[55] K. X. Rodriguez *et al.*, “Combined Scaffold Evaluation and Systems-Level Transcriptome-Based Analysis for Accelerated Lead Optimization Reveals Ribosomal Targeting Spirooxindole Cyclopropanes,” *ChemMedChem*, vol. 14, no. 18, pp. 1653–1661, 2019, doi: 10.1002/cmdc.201900266.

[56] M. Gladstone and T. T. Su, “Chemical genetics and drug screening in Drosophila cancer models,” *J Genet Genomics*, vol. 38, no. 10, pp. 497–504, Oct. 2011, doi: 10.1016/j.jgg.2011.09.003.

[57] K. Basler and G. Struhl, “Compartment boundaries and the control of Drosopfiffa limb pattern by hedgehog protein,” *Nature*, vol. 368, no. 6468, Art. no. 6468, Mar. 1994, doi: 10.1038/368208a0.

[58] M. Strigini and S. M. Cohen, “Wingless gradient formation in the Drosophila wing,” *Curr Biol*, vol. 10, no. 6, pp. 293–300, Mar. 2000, doi: 10.1016/s0960-9822(00)00378-x.

[59] D. Nellen, R. Burke, G. Struhl, and K. Basler, “Direct and Long-Range Action of a DPP Morphogen Gradient,” *Cell*, vol. 85, no. 3, pp. 357–368, May 1996, doi: 10.1016/S0092-8674(00)81114-9.

[60] A. Ratnaparkhi, S. Banerjee, and G. Hasan, “Altered Levels of Gq Activity Modulate Axonal Pathfinding inDrosophila,” *J. Neurosci.*, vol. 22, no. 11, pp. 4499–4508, Jun. 2002, doi: 10.1523/JNEUROSCI.22-11-04499.2002.

[61] E.-M. Ha *et al.*, “Regulation of DUOX by the Galphaq-phospholipase Cbeta-Ca2+ pathway in Drosophila gut immunity,” *Dev Cell*, vol. 16, no. 3, pp. 386–397, Mar. 2009, doi: 10.1016/j.devcel.2008.12.015.

[62] K. Venkatesh and G. Hasan, “Disruption of the IP3 receptor gene of Drosophila affects larval metamorphosis and ecdysone release,” *Current Biology*, vol. 7, no. 7, pp. 500–509, Jul. 1997, doi: 10.1016/S0960-9822(06)00221-1.

[63] X.-L. Kang, Y.-X. Li, Y.-L. Li, J.-X. Wang, and X.-F. Zhao, “The homotetramerization of a GPCR transmits the 20-hydroxyecdysone signal and increases its entry into cells for insect metamorphosis,” *Development*, vol. 148, no. 5, p. dev196667, 2021.

[64] X.-L. Kang *et al.*, “The steroid hormone 20-hydroxyecdysone binds to dopamine receptor to repress lepidopteran insect feeding and promote pupation,” *PLOS Genetics*, vol. 15, no. 8, p. e1008331, Aug. 2019, doi: 10.1371/journal.pgen.1008331.

[65] W. Liu, M.-J. Cai, J.-X. Wang, and X.-F. Zhao, “In a Nongenomic Action, Steroid Hormone 20-Hydroxyecdysone Induces Phosphorylation of Cyclin-Dependent Kinase 10 to Promote Gene Transcription,” *Endocrinology*, vol. 155, no. 5, pp. 1738–1750, May 2014, doi: 10.1210/en.2013-2020.

[66] D. P. Srivastava *et al.*, “Rapid, Nongenomic Responses to Ecdysteroids and Catecholamines Mediated by a Novel Drosophila G-Protein-Coupled Receptor,” *J.*

*Neurosci.*, vol. 25, no. 26, pp. 6145–6155, Jun. 2005, doi: 10.1523/JNEUROSCI.1005-05.2005.

[67] P. A. Brodskiy *et al.*, "Decoding Calcium Signaling Dynamics during Drosophila Wing Disc Development," *Biophysical Journal*, vol. 116, no. 4, pp. 725–740, Feb. 2019, doi: 10.1016/j.bpj.2019.01.007.

[68] C. K. Mirth, J. W. Truman, and L. M. Riddiford, "The Ecdysone receptor controls the post-critical weight switch to nutrition-independent differentiation in *Drosophila* wing imaginal discs," *Development*, vol. 136, no. 14, pp. 2345–2353, Jul. 2009, doi: 10.1242/dev.032672.

[69] J. Capdevila and I. Guerrero, "Targeted expression of the signaling molecule decapentaplegic induces pattern duplications and growth alterations in Drosophila wings.," *EMBO J*, vol. 13, no. 19, pp. 4459–4468, Oct. 1994.

[70] G. Schwank, S. Restrepo, and K. Basler, "Growth regulation by Dpp: an essential role for Brinker and a non-essential role for graded signaling levels," *Development*, vol. 135, no. 24, pp. 4003–4013, Dec. 2008, doi: 10.1242/dev.025635.

[71] F. J. Cifuentes and A. García-Bellido, "Proximo–distal specification in the wing disc of Drosophila by the nubbin gene," *PNAS*, vol. 94, no. 21, pp. 11405–11410, Oct. 1997, doi: 10.1073/pnas.94.21.11405.

[72] Y. Emori *et al.*, "Drosophila phospholipase C-gamma expressed predominantly in blastoderm cells at cellularization and in endodermal cells during later embryonic stages.," *Journal of Biological Chemistry*, vol. 269, no. 30, pp. 19474–19479, Jul. 1994, doi: 10.1016/S0021-9258(17)32193-2.

[73] M. Vervoort, M. Crozatier, D. Valle, and A. Vincent, "The COE transcription factor Collier is a mediator of short-range Hedgehog-induced patterning of the Drosophila wing," *Current Biology*, vol. 9, no. 12, pp. 632–639, Jun. 1999, doi: 10.1016/S0960-9822(99)80285-1.

[74] M. Strigini and S. M. Cohen, “A Hedgehog activity gradient contributes to AP axial patterning of the Drosophila wing,” *Development*, vol. 124, no. 22, Art. no. 22, Nov. 1997.

[75] A. Strasser, L. O’Connor, and V. M. Dixit, “Apoptosis Signaling,” *Annual Review of Biochemistry*, vol. 69, no. 1, pp. 217–245, 2000, doi: 10.1146/annurev.biochem.69.1.217.

[76] B. A. Hay, T. Wolff, and G. M. Rubin, “Expression of baculovirus P35 prevents cell death in Drosophila,” *Development*, vol. 120, no. 8, pp. 2121–2129, Aug. 1994.

[77] D. Christesen *et al.*, “Transcriptome Analysis of Drosophila melanogaster Third Instar Larval Ring Glands Points to Novel Functions and Uncovers a Cytochrome p450 Required for Development,” *G3 Genes|Genomes|Genetics*, vol. 7, no. 2, pp. 467–479, Feb. 2017, doi: 10.1534/g3.116.037333.

[78] M. e. Akam and J. r. Carlson, “The detection of Jonah gene transcripts in Drosophila by in situ hybridization.,” *The EMBO Journal*, vol. 4, no. 1, pp. 155–161, Jan. 1985, doi: 10.1002/j.1460-2075.1985.tb02330.x.

[79] J. Tower, “Heat shock proteins and Drosophila aging,” *Experimental Gerontology*, vol. 46, no. 5, pp. 355–362, May 2011, doi: 10.1016/j.exger.2010.09.002.

[80] H. R. B. Pelham, “Speculations on the functions of the major heat shock and glucose-regulated proteins,” *Cell*, vol. 46, no. 7, pp. 959–961, Sep. 1986, doi: 10.1016/0092-8674(86)90693-8.

[81] J. H. Feder, J. M. Rossi, J. Solomon, N. Solomon, and S. Lindquist, “The consequences of expressing hsp70 in Drosophila cells at normal temperatures.,” *Genes Dev.*, vol. 6, no. 8, pp. 1402–1413, Aug. 1992, doi: 10.1101/gad.6.8.1402.

[82] J. P. Charles, “The regulation of expression of insect cuticle protein genes,” *Insect Biochemistry and Molecular Biology*, vol. 40, no. 3, pp. 205–213, Mar. 2010, doi: 10.1016/j.ibmb.2009.12.005.

[83] A. Garelli, A. M. Gontijo, V. Miguela, E. Caparros, and M. Dominguez, “Imaginal Discs Secrete Insulin-Like Peptide 8 to Mediate Plasticity of Growth and Maturation,” *Science*, vol. 336, no. 6081, pp. 579–582, May 2012, doi: 10.1126/science.1216735.

[84] J. Colombani, D. S. Andersen, and P. Léopold, “Secreted Peptide Dilp8 Coordinates Drosophila Tissue Growth with Developmental Timing,” *Science*, vol. 336, no. 6081, pp. 582–585, May 2012, doi: 10.1126/science.1216689.

[85] W. A. Segraves and D. S. Hogness, “The E75 ecdysone-inducible gene responsible for the 75B early puff in Drosophila encodes two new members of the steroid receptor superfamily.,” *Genes Dev.*, vol. 4, no. 2, pp. 204–219, Feb. 1990, doi: 10.1101/gad.4.2.204.

[86] L. G. Wright, T. Chen, C. S. Thummel, and G. M. Guild, “Molecular Characterization of the 71E Late Puff inDrosophila melanogasterReveals a Family of Novel Genes,” *Journal of Molecular Biology*, vol. 255, no. 3, pp. 387–400, Jan. 1996, doi: 10.1006/jmbi.1996.0032.

[87] N. Okamoto *et al.*, “A Membrane Transporter Is Required for Steroid Hormone Uptake in Drosophila,” *Developmental Cell*, vol. 47, no. 3, pp. 294-305.e7, Nov. 2018, doi: 10.1016/j.devcel.2018.09.012.

[88] A. C. Ghosh, Y. Hu, S. G. Tattikota, Y. Liu, A. Comjean, and N. Perrimon, “Modeling exercise using optogenetically contractible Drosophila larvae,” *BMC Genomics*, vol. 23, no. 1, p. 623, Aug. 2022, doi: 10.1186/s12864-022-08845-6.

[89] F. Germani, D. Hain, D. Sternlicht, E. Moreno, and K. Basler, “The Toll pathway inhibits tissue growth and regulates cell fitness in an infection-dependent manner,” *eLife*, vol. 7, p. e39939, Nov. 2018, doi: 10.7554/eLife.39939.

[90] T. Kawasaki and T. Kawai, “Toll-Like Receptor Signaling Pathways,” *Frontiers in Immunology*, vol. 5, 2014, Accessed: Aug. 15, 2022. [Online]. Available: https://www.frontiersin.org/articles/10.3389/fimmu.2014.00461

[91] L. Alpar, C. Bergantiños, and L. A. Johnston, “Spatially Restricted Regulation of Spätzle/Toll Signaling during Cell Competition,” *Developmental Cell*, vol. 46, no. 6, pp. 706-719.e5, Sep. 2018, doi: 10.1016/j.devcel.2018.08.001.

[92] B. Lemaitre and J. Hoffmann, Eds., “The host defense of Drosophila melanogaster,” *Annual review of immunology*, 2007, doi: 10.1146/annurev.immunol.25.022106.141615.

[93] Z. Kambris *et al.*, “Drosophila immunity: a large-scale in vivo RNAi screen identifies five serine proteases required for Toll activation,” *Curr Biol*, vol. 16, no. 8, pp. 808–813, Apr. 2006, doi: 10.1016/j.cub.2006.03.020.

[94] B. Lemaitre, E. Nicolas, L. Michaut, J.-M. Reichhart, and J. A. Hoffmann, “The Dorsoventral Regulatory Gene Cassette spätzle/Toll/cactus Controls the Potent Antifungal Response in Drosophila Adults,” *Cell*, vol. 86, no. 6, pp. 973–983, Sep. 1996, doi: 10.1016/S0092-8674(00)80172-5.

[95] Y. T. Ip *et al.*, “Dif, a dorsal-related gene that mediates an immune response in Drosophila,” *Cell*, vol. 75, no. 4, pp. 753–763, Nov. 1993, doi: 10.1016/0092-8674(93)90495-C.

[96] S. W. Roth, M. D. Bitterman, M. J. Birnbaum, and M. L. Bland, “Innate Immune Signaling in Drosophila Blocks Insulin Signaling by Uncoupling PI(3,4,5)P3 Production and Akt Activation,” *Cell Reports*, vol. 22, no. 10, pp. 2550–2556, Mar. 2018, doi: 10.1016/j.celrep.2018.02.033.

[97] M. S. Dionne, L. N. Pham, M. Shirasu-Hiza, and D. S. Schneider, “Akt and foxo Dysregulation Contribute to Infection-Induced Wasting in Drosophila,” *Current Biology*, vol. 16, no. 20, pp. 1977–1985, Oct. 2006, doi: 10.1016/j.cub.2006.08.052.

[98] J. R. DiAngelo, M. L. Bland, S. Bambina, S. Cherry, and M. J. Birnbaum, “The immune response attenuates growth and nutrient storage in Drosophila by reducing insulin signaling,” *Proceedings of the National Academy of Sciences*, vol. 106, no. 49, pp. 20853–20858, Dec. 2009, doi: 10.1073/pnas.0906749106.

[99] D. A. Harrison, P. E. McCoon, R. Binari, M. Gilman, and N. Perrimon, “Drosophila unpaired encodes a secreted protein that activates the JAK signaling pathway,” *Genes Dev.*, vol. 12, no. 20, pp. 3252–3263, Oct. 1998, doi: 10.1101/gad.12.20.3252.

[100] H. Luo and C. R. Dearolf, “The JAK/STAT pathway and Drosophila development,” *BioEssays*, vol. 23, no. 12, pp. 1138–1147, 2001, doi: 10.1002/bies.10016.

[101] V. M. Wright, K. L. Vogt, E. Smythe, and M. P. Zeidler, “Differential activities of the Drosophila JAK/STAT pathway ligands Upd, Upd2 and Upd3,” *Cellular Signalling*, vol. 23, no. 5, pp. 920–927, May 2011, doi: 10.1016/j.cellsig.2011.01.020.

[102] M. S. Flaherty *et al.*, “chinmo Is a Functional Effector of the JAK/STAT Pathway that Regulates Eye Development, Tumor Formation, and Stem Cell Self-Renewal in Drosophila,” *Developmental Cell*, vol. 18, no. 4, pp. 556–568, Apr. 2010, doi: 10.1016/j.devcel.2010.02.006.

[103] T. Katsuyama, F. Comoglio, M. Seimiya, E. Cabuy, and R. Paro, “During Drosophila disc regeneration, JAK/STAT coordinates cell proliferation with Dilp8-mediated developmental delay,” *Proceedings of the National Academy of Sciences*, vol. 112, no. 18, pp. E2327–E2336, May 2015, doi: 10.1073/pnas.1423074112.

[104] M. Li, S. Sun, J. Priest, X. Bi, and Y. Fan, “Characterization of TNF-induced cell death in Drosophila reveals caspase- and JNK-dependent necrosis and its role in tumor suppression,” *Cell Death Dis*, vol. 10, no. 8, Art. no. 8, Aug. 2019, doi: 10.1038/s41419-019-1862-0.

[105] J. E. La Marca and H. E. Richardson, “Two-Faced: Roles of JNK Signalling During Tumourigenesis in the Drosophila Model,” *Frontiers in Cell and Developmental Biology*, vol. 8, 2020, Accessed: Nov. 28, 2022. [Online]. Available: https://www.frontiersin.org/articles/10.3389/fcell.2020.00042

[106] G. Lavorgna, F. D. Karim, C. S. Thummel, and C. Wu, “Potential role for a FTZ-F1 steroid receptor superfamily member in the control of Drosophila metamorphosis.,” *Proceedings*

*of the National Academy of Sciences*, vol. 90, no. 7, pp. 3004–3008, Apr. 1993, doi: 10.1073/pnas.90.7.3004.

[107] M. Schubiger, A. A. Wade, G. E. Carney, J. W. Truman, and M. Bender, "Drosophila EcR-B ecdysone receptor isoforms are required for larval molting and for neuron remodeling during metamorphosis," *Development*, vol. 125, no. 11, pp. 2053–2062, Jun. 1998, doi: 10.1242/dev.125.11.2053.

[108] W. S. Talbot, E. A. Swyryd, and D. S. Hogness, "Drosophila tissues with different metamorphic responses to ecdysone express different ecdysone receptor isoforms," *Cell*, vol. 73, no. 7, pp. 1323–1337, Jul. 1993, doi: 10.1016/0092-8674(93)90359-X.

[109] M. R. Koelle, W. S. Talbot, W. A. Segraves, M. T. Bender, P. Cherbas, and D. S. Hogness, "The drosophila EcR gene encodes an ecdysone receptor, a new member of the steroid receptor superfamily," *Cell*, vol. 67, no. 1, pp. 59–77, Oct. 1991, doi: 10.1016/0092-8674(91)90572-G.

[110] A. A. Sullivan and C. S. Thummel, "Temporal Profiles of Nuclear Receptor Gene Expression Reveal Coordinate Transcriptional Responses during Drosophila Development," *Molecular Endocrinology*, vol. 17, no. 11, pp. 2125–2137, Nov. 2003, doi: 10.1210/me.2002-0430.

[111] C. Justet, J. A. Hernández, A. Torriglia, and S. Chifflet, "Fast calcium wave inhibits excessive apoptosis during epithelial wound healing," *Cell and tissue research*, vol. 365, no. 2, Art. no. 2, 2016.

[112] F. Saad and D. R. Hipfner, "Extensive crosstalk of G protein-coupled receptors with the Hedgehog signalling pathway," *Development*, vol. 148, no. 7, p. dev189258, Apr. 2021, doi: 10.1242/dev.189258.

[113] N. Katanayeva, D. Kopein, R. Portmann, D. Hess, and V. L. Katanaev, "Competing Activities of Heterotrimeric G Proteins in Drosophila Wing Maturation," *PLOS ONE*, vol. 5, no. 8, p. e12331, Aug. 2010, doi: 10.1371/journal.pone.0012331.

[114] L. F. Sobala and P. N. Adler, “The Gene Expression Program for the Formation of Wing Cuticle in Drosophila,” *PLOS Genetics*, vol. 12, no. 5, p. e1006100, May 2016, doi: 10.1371/journal.pgen.1006100.

[115] D. Y. Jhon *et al.*, “Cloning, sequencing, purification, and Gq-dependent activation of phospholipase C-beta 3,” *J Biol Chem*, vol. 268, no. 9, pp. 6654–6661, Mar. 1993.

[116] C. W. Lee, K. H. Lee, S. B. Lee, D. Park, and S. G. Rhee, “Regulation of phospholipase C-beta 4 by ribonucleotides and the alpha subunit of Gq.,” *Journal of Biological Chemistry*, vol. 269, no. 41, pp. 25335–25338, Oct. 1994, doi: 10.1016/S0021-9258(18)47252-3.

[117] S. Banerjee *et al.*, “Compensation of Inositol 1,4,5-Trisphosphate Receptor Function by Altering Sarco-Endoplasmic Reticulum Calcium ATPase Activity in the Drosophila Flight Circuit,” *J. Neurosci.*, vol. 26, no. 32, pp. 8278–8288, Aug. 2006, doi: 10.1523/JNEUROSCI.1231-06.2006.

[118] H. Streb, R. F. Irvine, M. J. Berridge, and I. Schulz, “Release of Ca2+ from a nonmitochondrial intracellular store in pancreatic acinar cells by inositol-1,4,5-trisphosphate,” *Nature*, vol. 306, no. 5938, Art. no. 5938, Nov. 1983, doi: 10.1038/306067a0.

[119] T. Furuichi, S. Yoshikawa, A. Miyawaki, K. Wada, N. Maeda, and K. Mikoshiba, “Primary structure and functional expression of the inositol 1,4,5-trisphosphate-binding protein P400,” *Nature*, vol. 342, no. 6245, Art. no. 6245, Nov. 1989, doi: 10.1038/342032a0.

[120] M. J. Berridge and R. F. Irvine, “Inositol trisphosphate, a novel second messenger in cellular signal transduction,” *Nature*, vol. 312, no. 5992, pp. 315–321, Nov. 1984, doi: 10.1038/312315a0.

[121] G. Sánchez-Fernández *et al.*, “Gαq signalling: The new and the old,” *Cellular Signalling*, vol. 26, no. 5, pp. 833–848, May 2014, doi: 10.1016/j.cellsig.2014.01.010.

[122] "Cooperative mitogenic signaling by G protein-coupled receptors and growth factors is dependent on Gq/11", doi: 10.1096/fj.05-5622fje.

[123] D. Zindel *et al.*, "G protein-coupled receptors can control the Hippo/YAP pathway through Gq signaling," *The FASEB Journal*, vol. 35, no. 7, p. e21668, 2021, doi: 10.1096/fj.202002159R.

[124] A. L. Howes, S. Miyamoto, J. W. Adams, E. A. Woodcock, and J. H. Brown, "Gαq expression activates EGFR and induces Akt mediated cardiomyocyte survival: dissociation from Gαq mediated hypertrophy," *Journal of Molecular and Cellular Cardiology*, vol. 40, no. 5, pp. 597–604, May 2006, doi: 10.1016/j.yjmcc.2005.12.003.

[125] G. Nadel, Z. Yao, I. Ben-Ami, Z. Naor, and R. Seger, "Gq-Induced Apoptosis is Mediated by AKT Inhibition That Leads to PKC-Induced JNK Activation," *Cell Physiol Biochem*, vol. 50, no. 1, pp. 121–135, 2018, doi: 10.1159/000493963.

[126] C. Justet, J. A. Hernández, A. Torriglia, and S. Chifflet, "Fast calcium wave inhibits excessive apoptosis during epithelial wound healing," *Cell Tissue Res*, vol. 365, no. 2, pp. 343–356, Aug. 2016, doi: 10.1007/s00441-016-2388-8.

[127] M. P. Zeidler, E. A. Bach, and N. Perrimon, "The roles of the Drosophila JAK/STAT pathway," *Oncogene*, vol. 19, no. 21, Art. no. 21, May 2000, doi: 10.1038/sj.onc.1203482.

[128] S. Ekengren and D. Hultmark, "A Family of Turandot-Related Genes in the Humoral Stress Response of Drosophila," *Biochemical and Biophysical Research Communications*, vol. 284, no. 4, pp. 998–1003, Jun. 2001, doi: 10.1006/bbrc.2001.5067.

[129] R. Eferl and E. F. Wagner, "AP-1: a double-edged sword in tumorigenesis," *Nat Rev Cancer*, vol. 3, no. 11, Art. no. 11, Nov. 2003, doi: 10.1038/nrc1209.

[130] M. La Fortezza, M. Schenk, A. Cosolo, A. Kolybaba, I. Grass, and A.-K. Classen, "JAK/STAT signalling mediates cell survival in response to tissue stress," *Development*, vol. 143, no. 16, pp. 2907–2919, Aug. 2016, doi: 10.1242/dev.132340.

[131] J. S. Jaszczak, J. B. Wolpe, R. Bhandari, R. G. Jaszczak, and A. Halme, "Growth Coordination During Drosophila melanogaster Imaginal Disc Regeneration Is Mediated by Signaling Through the Relaxin Receptor Lgr3 in the Prothoracic Gland," *Genetics*, vol. 204, no. 2, pp. 703–709, Oct. 2016, doi: 10.1534/genetics.116.193706.

[132] E. H. T. Wu, R. K. H. Lo, and Y. H. Wong, "Regulation of STAT3 activity by G16-coupled receptors," *Biochemical and Biophysical Research Communications*, vol. 303, no. 3, pp. 920–925, Apr. 2003, doi: 10.1016/S0006-291X(03)00451-0.

[133] P. T. Ram, C. M. Horvath, and R. Iyengar, "Stat3-Mediated Transformation of NIH-3T3 Cells by the Constitutively Active Q205L Gαo Protein," *Science*, vol. 287, no. 5450, pp. 142–144, Jan. 2000, doi: 10.1126/science.287.5450.142.

[134] L. Bellocchio *et al.*, "Sustained Gq-Protein Signaling Disrupts Striatal Circuits via JNK," *J. Neurosci.*, vol. 36, no. 41, pp. 10611–10624, Oct. 2016, doi: 10.1523/JNEUROSCI.1192-16.2016.

[135] J. P. Vaqué *et al.*, "A Genome-wide RNAi Screen Reveals a Trio-Regulated Rho GTPase Circuitry Transducing Mitogenic Signals Initiated by G Protein-Coupled Receptors," *Molecular Cell*, vol. 49, no. 1, pp. 94–108, Jan. 2013, doi: 10.1016/j.molcel.2012.10.018.

[136] X. Liang *et al.*, "Arabidopsis heterotrimeric G proteins regulate immunity by directly coupling to the FLS2 receptor," *eLife*, vol. 5, p. e13568, Apr. 2016, doi: 10.7554/eLife.13568.

[137] L. Zhang and G. Shi, "Gq-Coupled Receptors in Autoimmunity," *Journal of Immunology Research*, vol. 2016, p. e3969023, Jan. 2016, doi: 10.1155/2016/3969023.

[138] H. Qian *et al.*, "Role of Galphaq in pathogenesis of psoriasis, a new mechanism about the immune regulation in psoriasis," *International Immunopharmacology*, vol. 68, pp. 185–192, Mar. 2019, doi: 10.1016/j.intimp.2018.12.054.

[139] H. Zhu *et al.*, "Arabidopsis Extra Large G-Protein 2 (XLG2) Interacts with the Gβ Subunit of Heterotrimeric G Protein and Functions in Disease Resistance," *Molecular Plant*, vol. 2, no. 3, pp. 513–525, May 2009, doi: 10.1093/mp/ssp001.

[140] F. Saad and D. R. Hipfner, "Extensive crosstalk of G protein-coupled receptors with the Hedgehog signalling pathway," *Development*, vol. 148, no. 7, p. dev189258, Apr. 2021, doi: 10.1242/dev.189258.

[141] Z. ZhengHong and Z. Ru, "Research progress on the longevity gene methuselah in Drosophila.," *Acta Entomologica Sinica*, vol. 55, no. 12, pp. 1394–1398, 2012.

[142] Y.-L. Li *et al.*, "Identification and Functional Analysis of G Protein-Coupled Receptors in 20-Hydroxyecdysone Signaling From the Helicoverpa armigera Genome," *Frontiers in cell and developmental biology*, vol. 9, 2021.

[143] T. Mukherjee, U. Schäfer, and M. P. Zeidler, "Identification of Drosophila Genes Modulating Janus Kinase/Signal Transducer and Activator of Transcription Signal Transduction," *Genetics*, vol. 172, no. 3, pp. 1683–1697, Mar. 2006, doi: 10.1534/genetics.105.046904.

[144] Y.-J. I. Jong, S. K. Harmon, and K. L. O'Malley, "GPCR signalling from within the cell," *British Journal of Pharmacology*, vol. 175, no. 21, pp. 4026–4035, 2018, doi: 10.1111/bph.14023.

[145] I. Fasciani *et al.*, "GPCRs in Intracellular Compartments: New Targets for Drug Discovery," *Biomolecules*, vol. 12, no. 10, Art. no. 10, Oct. 2022, doi: 10.3390/biom12101343.

[146] M. Friedrich and J. W. Jones, "Gene Ages, Nomenclatures, and Functional Diversification of the Methuselah/Methuselah-Like GPCR Family in Drosophila and Tribolium," *Journal of Experimental Zoology Part B: Molecular and Developmental Evolution*, vol. 326, no. 8, pp. 453–463, 2016, doi: 10.1002/jez.b.22721.

[147] A. M. Bolger, M. Lohse, and B. Usadel, “Trimmomatic: a flexible trimmer for Illumina sequence data,” *Bioinformatics*, vol. 30, no. 15, pp. 2114–2120, Aug. 2014, doi: 10.1093/bioinformatics/btu170.

[148] “Babraham Bioinformatics - FastQC A Quality Control tool for High Throughput Sequence Data.” https://www.bioinformatics.babraham.ac.uk/projects/fastqc/ (accessed Feb. 16, 2022).

[149] D. Kim, J. M. Paggi, C. Park, C. Bennett, and S. L. Salzberg, “Graph-based genome alignment and genotyping with HISAT2 and HISAT-genotype,” *Nat Biotechnol*, vol. 37, no. 8, Art. no. 8, Aug. 2019, doi: 10.1038/s41587-019-0201-4.

[150] H. Li *et al.*, “The Sequence Alignment/Map format and SAMtools,” *Bioinformatics*, vol. 25, no. 16, pp. 2078–2079, Aug. 2009, doi: 10.1093/bioinformatics/btp352.

[151] S. Anders, P. T. Pyl, and W. Huber, “HTSeq--a Python framework to work with high-throughput sequencing data,” *Bioinformatics*, vol. 31, no. 2, pp. 166–169, Jan. 2015, doi: 10.1093/bioinformatics/btu638.

[152] M. D. Robinson, D. J. McCarthy, and G. K. Smyth, “edgeR: a Bioconductor package for differential expression analysis of digital gene expression data,” *Bioinformatics*, vol. 26, no. 1, pp. 139–140, Jan. 2010, doi: 10.1093/bioinformatics/btp616.

[153] M. D. Robinson and G. K. Smyth, “Small-sample estimation of negative binomial dispersion, with applications to SAGE data,” *Biostatistics*, vol. 9, no. 2, pp. 321–332, Jul. 2007, doi: 10.1093/biostatistics/kxm030.

[154] M. D. Robinson and G. K. Smyth, “Moderated statistical tests for assessing differences in tag abundance,” *Bioinformatics*, vol. 23, no. 21, pp. 2881–2887, Nov. 2007, doi: 10.1093/bioinformatics/btm453.

[155] D. J. McCarthy, Y. Chen, and G. K. Smyth, “Differential expression analysis of multifactor RNA-Seq experiments with respect to biological variation,” *Nucleic Acids Research*, vol. 40, no. 10, pp. 4288–4297, May 2012, doi: 10.1093/nar/gks042.

[156] R. J. Kinsella *et al.*, “Ensembl BioMarts: a hub for data retrieval across taxonomic space,” *Database*, vol. 2011, no. 0, pp. bar030–bar030, Jul. 2011, doi: 10.1093/database/bar030.

[157] A. M. Gontijo and A. Garelli, “The biology and evolution of the Dilp8-Lgr3 pathway: A relaxin-like pathway coupling tissue growth and developmental timing control,” *Mechanisms of Development*, vol. 154, pp. 44–50, Dec. 2018, doi: 10.1016/j.mod.2018.04.005.

## List of Additional Files

- **Additional File 1**
  - Document (.pdf)
  - Supplementary text
  - This file includes the figure for the trichome analysis of the intervein areas. It also includes the figures of the results obtained from the GO enrichment analysis of the differentially expressed genes. In addition, it contains supplementary text for the methods used to analyze the wings and the methods used to plot the GO enrichment results.
- **Additional File 2**
  - spreadsheet (.csv)
  - Fold changes of differentially expressed genes associated with immune-related GO terms.
  - This file contains the fold changes of differentially expressed genes involved in immune response in response to both *Gαq* perturbations.
- **Additional File 3**
  - spreadsheet (.csv)
  - Differentially expressed genes between C765>Ryr$^{RNAi}$ and *C765>Gαq*$^{RNAi}$
  - This file contains the results of the differential gene expression analyses of the RNA sequencing data for *C765>Ryr*$^{RNAi}$ vs. *C765>Gαq*$^{RNAi}$.
- **Additional File 4**
  - spreadsheet (.csv)
  - Differentially expressed genes between C765>Ryr$^{RNAi}$ and *C765>Gαq*
  - This file contains the results of the differential gene expression analyses of the RNA sequencing data for *C765>Ryr*$^{RNAi}$ vs. *C765>Gαq*

# Figures

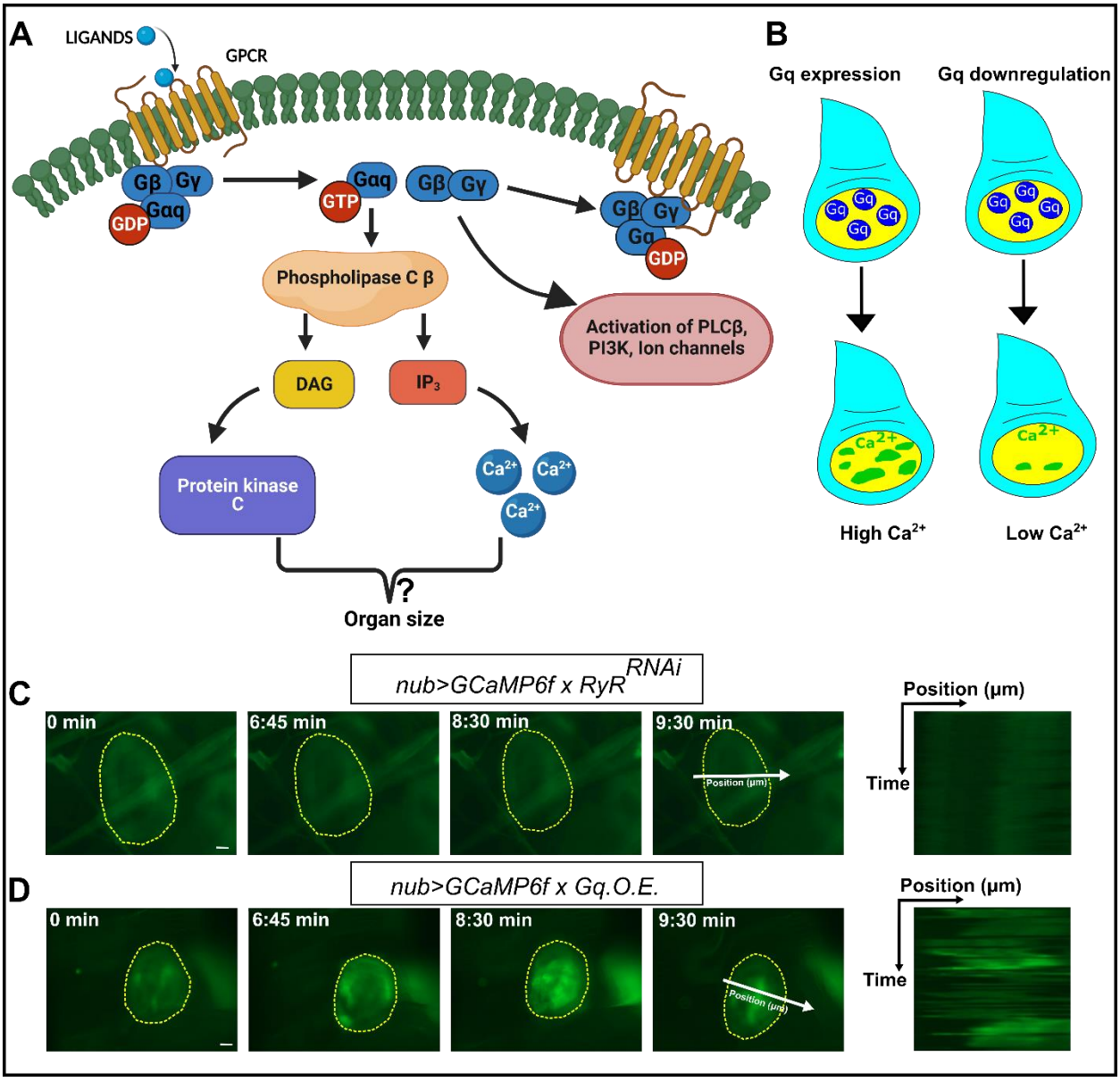


**Figure 1: Overexpression of Gq in the wing disc pouch is sufficient to generate periodic multicellular $Ca^{2+}$ transients and waves *in vivo*. A**) Schematic of G Protein signaling network (partial). Hetero-trimeric proteins Gα, Gβ, and Gγ form a complex when bound to GDP. When ligands bind to G protein-coupled receptors, the Gα dissociates from the complex by exchanging GDP with GTP. GTP-bound Gαq activates the Phospholipase C β enzyme to catalyze the conversion of $PIP_2$ to $IP_3$ and DAG. $IP_3$ binds to the $IP_3$ receptor on the endoplasmic reticulum

(ER), facilitating the release of stored $Ca^{2+}$ into the cytoplasm from ER. DAG activates PKC, which further activates cAMP and other downstream signaling effectors. **B**) Schematic of a wing disc expressing wild type *Gαq* (denoted as *Gαq. O.E*) in the wing disc pouch cells using a binary expression system. High expression levels of *Gαq* result in calcium transients and waves. **C**, **D**). Time-lapse images from *in vivo* imaging of wing discs expressing $RyR^{RNAi}$ and wildtype *Gαq* under the control of the nubbin (nub)-Gal4 driver, respectively. GCaMP6 sensor was co-expressed under the nub-Gal4 driver. Upregulation of *Gαq* in the wing disc results in the formation of periodic intercellular $Ca^{2+}$ waves *in vivo* (D). Minimal $Ca^{2+}$ activity, such as $Ca^{2+}$ spikes, was observed in control discs expressing nonsense $RyR^{RNAi}$ (C). Yellow dotted lines indicate the wing disc pouch boundary. The UAS lines are as follows: $Gαq^{WT}$, BDSC:30734, $RyR^{RNAi}$, BDSC:31540. Scale bars indicate 20 µm.

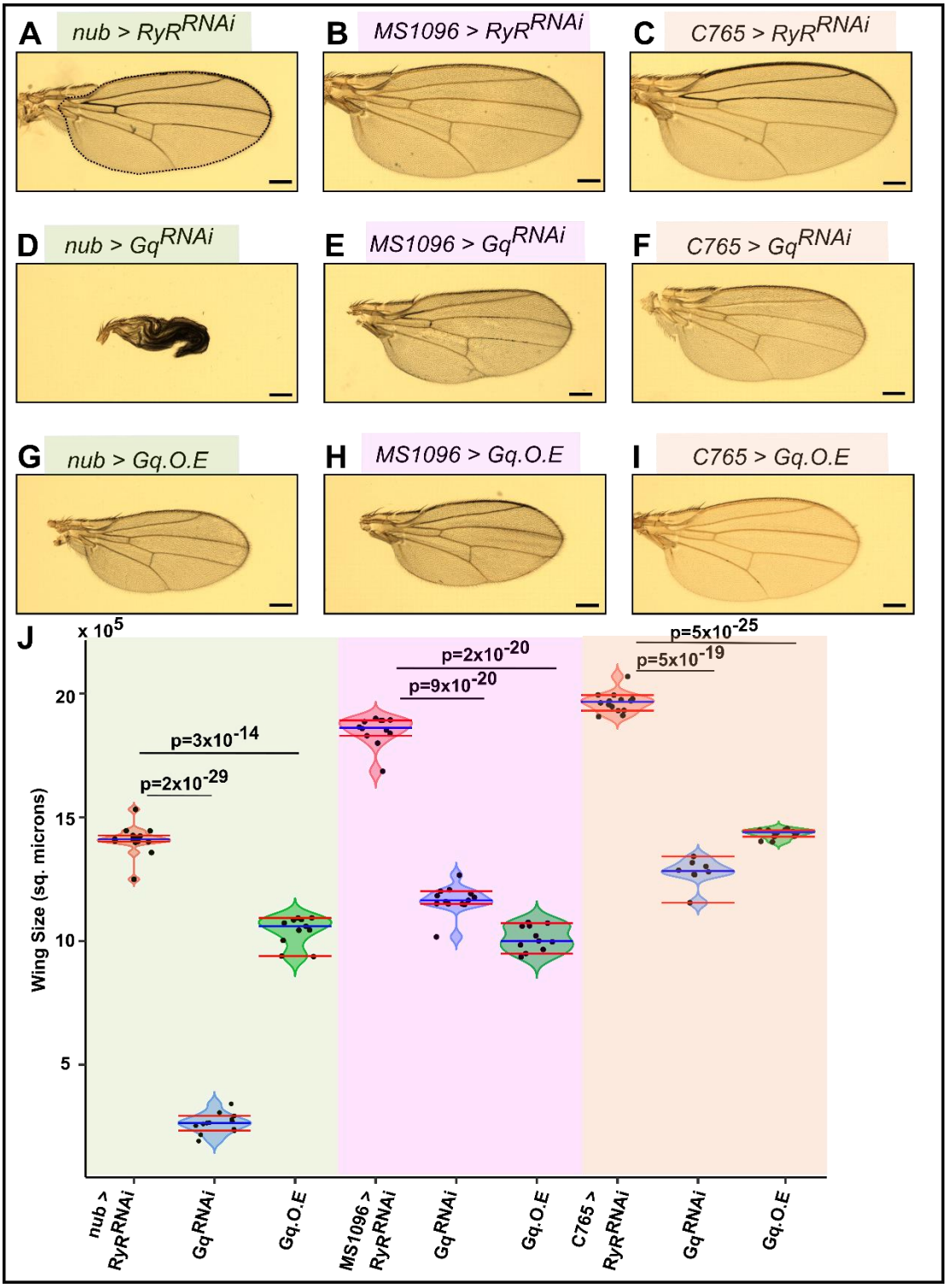


1431

1432 **Figure 2: Perturbing *Gαq* expression in the *Drosophila* wing disc decreases overall adult**

1433 **wing size and can prevent pupal wing expansion. A-I**) Micrographs of adult wings expressing

*RyR*$^{RNAi}$ (control), wild type *Gαq*, or *Gαq*$^{RNAi}$ under several GAL4 drivers, including nubbin, MS1096, and C765. **D-F**) Knockdown of *Gαq* leads to a reduction in wing size for multiple Gal4 drivers. RNAi-mediated inhibition of *Gαq* driven by the *nubbin-Gal4* driver led to severe pupal wing expansion phenotypes. **G-I**) *Gαq* overexpression leads to decreased wing size for multiple drivers. **J**) Graphs comparing the wing area for wings from the crosses indicated in (A-I). The blue line represents the median, and the red lines indicate the 95% confidence interval of the median. N > 10 for all samples shown except for *nub> Gαq*$^{RNAi}$ (n=8). The scale bar represents 100 microns. The blue line represents the median, and the red lines indicate the 95% confidence interval of the median. Student two-tailed t-test was used to determine the statistical significance.

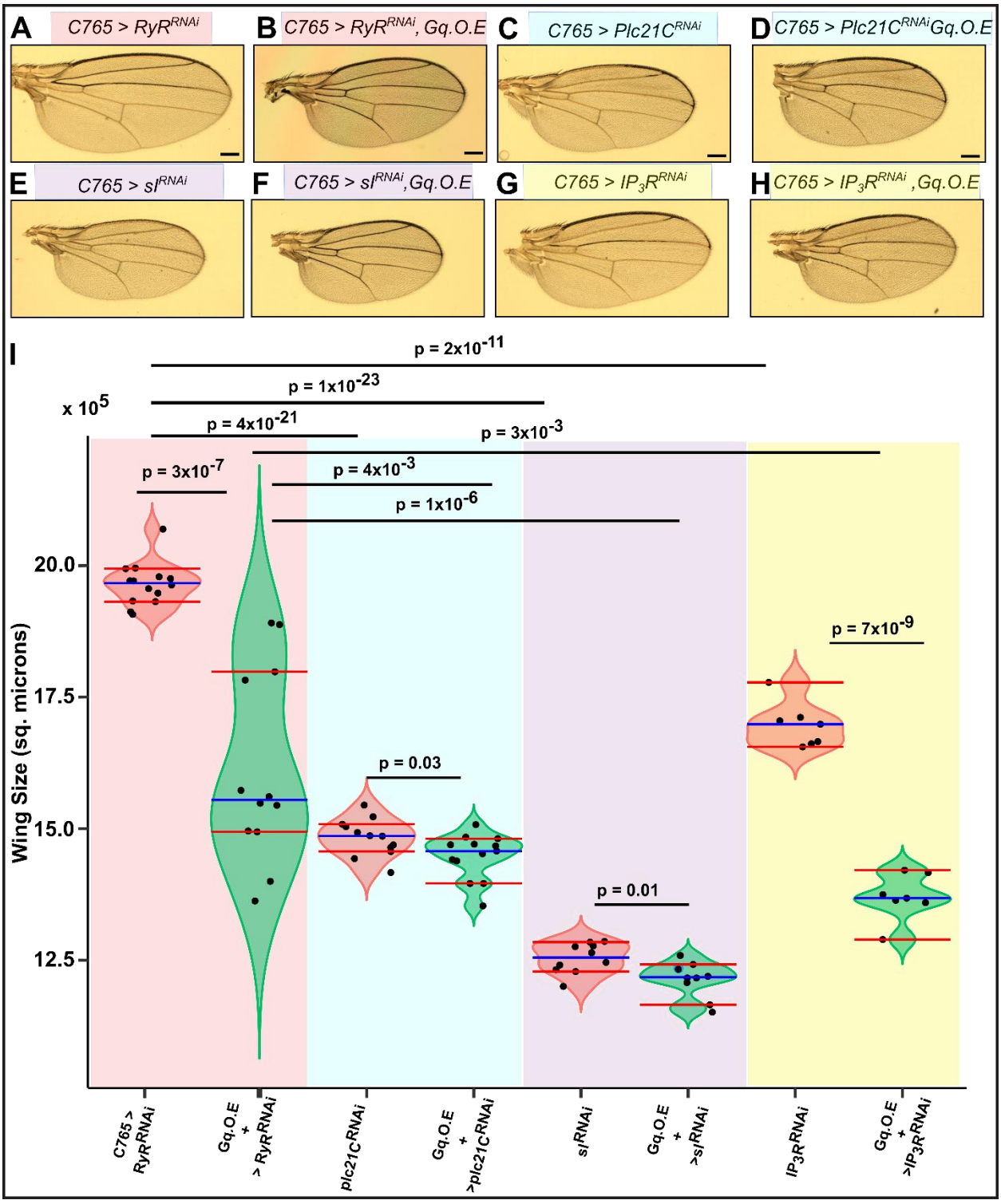


**Figure 3: *Gαq* overexpression, together with inhibition of $Ca^{2+}$ signaling components, results in further reduction of wing size. A-H**) Micrographs of adult wing images. Reduction in core $Ca^{2+}$ signaling components such as *plc21c*, *sl*, and *itpr* ($IP_3R$) through RNAi-mediated

knockdown in the wing disc results in a reduction of the size of the wings. Overexpressing wildtype *Gαq*, in combination with the knockdown of $Ca^{2+}$ signaling components, further decreases the size of the wings. **I**) Quantification of the adult wing blade areas for the crosses listed in (**A-H**). The blue line represents the median, and the red lines indicate the 95% confidence interval of the median. Scale bars are 100 µm. Student t-test was used to determine the statistical significance.

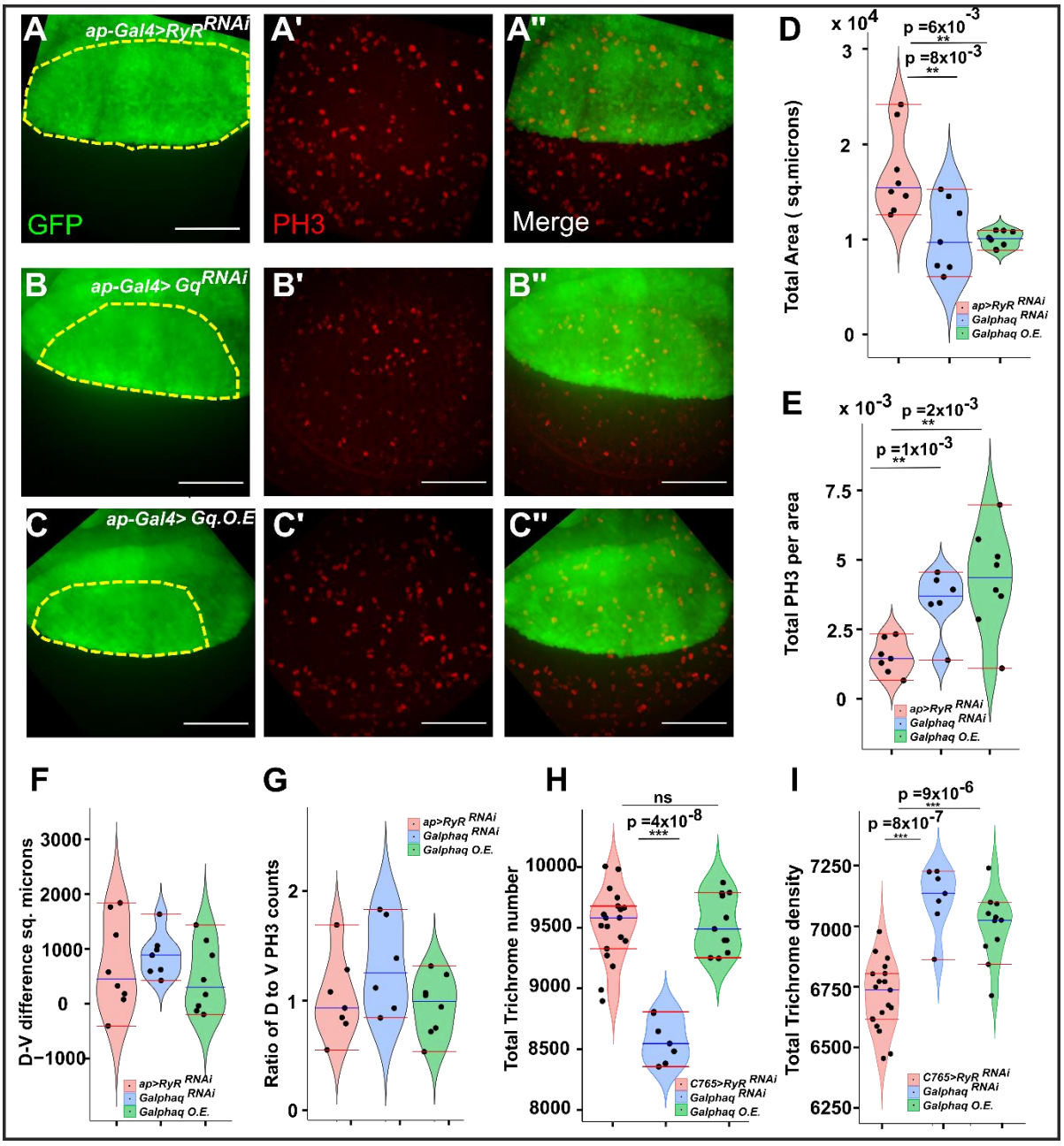


**Figure 4**: **Gαq homeostasis modulates the proliferation of wing disc and affects the overall cell number in the wing**. **A**, **B**, **C**) Representative images of wing discs stained with PH3 expressing RyR$^{RNAi}$, *Gαq*$^{WT,}$ and *Gαq* $^{RNAi}$ under the control of apterous. PH3 density was higher in the discs with *Gαq* overexpression and RNAi conditions when compared to the control. **D**) Violin plots comparing the total area of the wing pouch for *Gαq* perturbations with control. The pouch area was significantly reduced in the overexpression and RNAi conditions as compared to

the control condition. **E**) Violin plot showing the density of PH3 in the wing pouch for the control and *Gαq* perturbations. PH3 density was found to be higher in both *Gαq* overexpression and RNAi conditions. **F**) The violin plots illustrate the difference between the area of the dorsal and ventral regions of the wing discs under control and *Gαq* perturbations. **G**) There exists no difference in the number of PH3 cells in the dorsal and ventral regions for all the genetic perturbations. (n>5 for all conditions) **H**) Violin plot comparing trichome number between wings with *Gαq* overexpression, RNAi, and control conditions. Trichome number is significantly lower for wings with *Gαq* knockdown, whereas overexpression does not show any difference. **I**) Graphs comparing the total trichome densities for *Gαq* overexpression, $Gαq^{RNAi}$, and $RyR^{RNAi}$. Trichome density is significantly higher for both overexpression and RNAi conditions indicating that Gαq homeostasis affects the cell number during the growth of the wing disc.

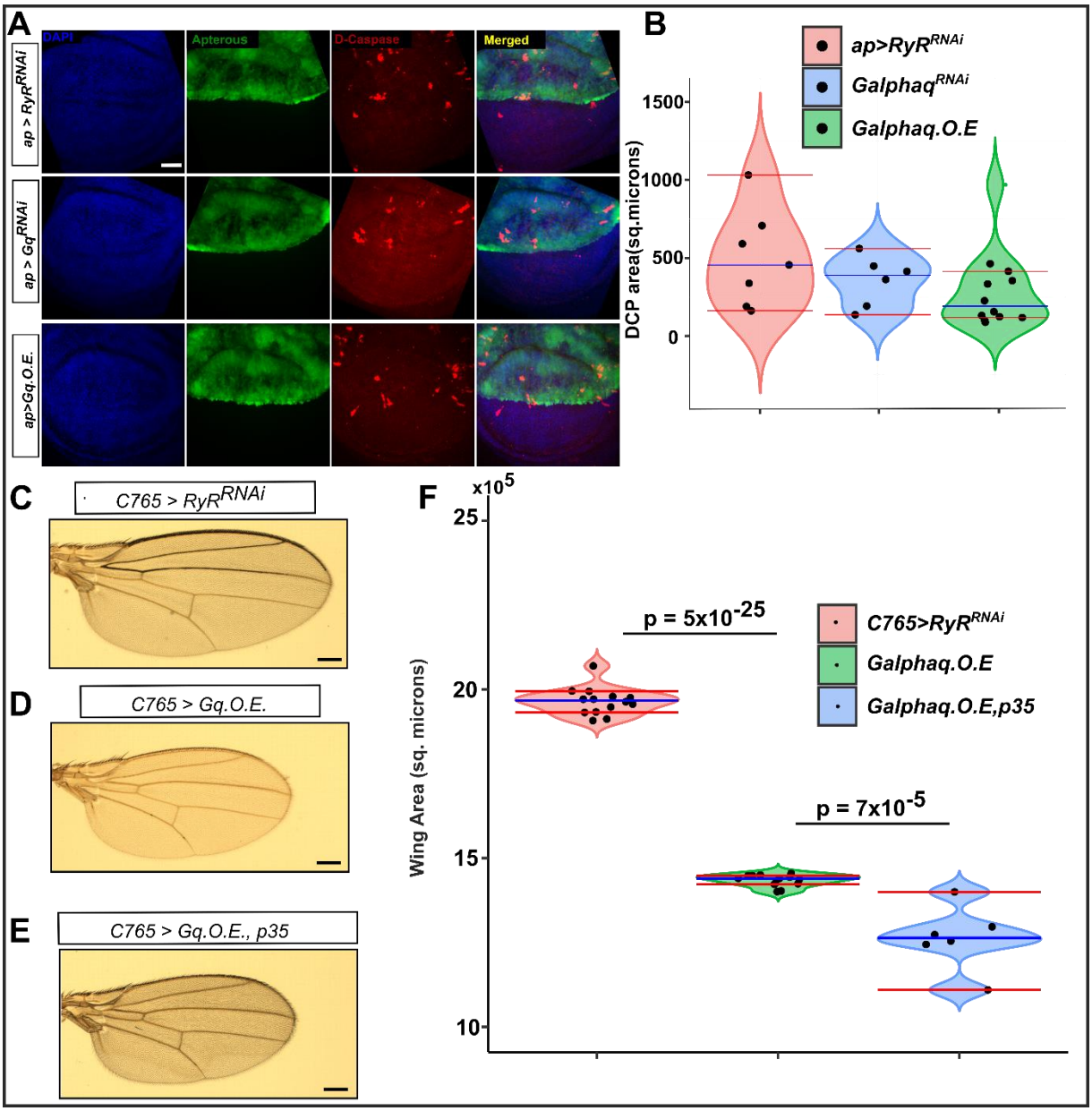


**Figure 5: Reduction in adult wing size for both *Gαq* overexpression and downregulation is not mediated by apoptosis. A**) Representative images of the third instar wing disc from the corresponding cross stained for Dcp-1 to show apoptotic cells. Wing discs were also stained with nuclear dye DAPI, and the region of GAL4 expression, which drives the *Gαq* perturbation, is indicated using GFP. All wing discs are positioned anterior to the right and posterior to the left. Sample sizes are n = 3 to 8 for each condition. **B**) Violin pot comparing the area of Dcp-1 stain for all three genotypes. **C-E**) Micrographs of adult wings. Genotypes of individual wings are given

on the top left. Ectopic expression of apoptosis inhibitor p35 did not rescue the size reduction defect caused by overexpression of *Gαq*. **F**) Quantification of the adult wing blade area from the indicated genotypes. Student t-test was performed, and the p-values are indicated on the plot. The blue line represents the median, and the red lines indicate the 95% confidence interval of the median. Scale bars represent 100 µm.

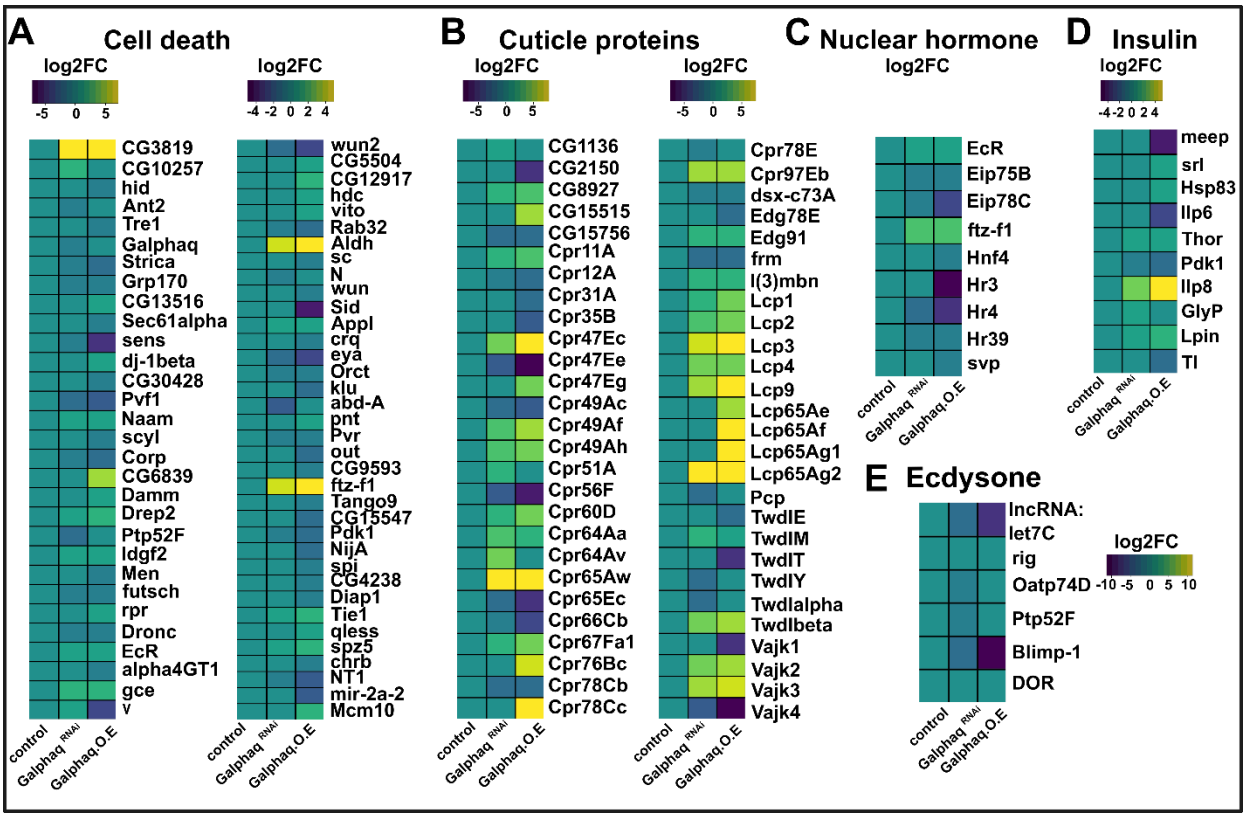


**Figure 6: Disruption of Gαq homeostasis delays development through transcriptional changes in multiple modules**

**A**) Transcriptomic analysis of genes related to programmed cell death for *Gαq* RNAi and *Gαq* overexpression. The apoptotic gene (*ftz-f1*) and Mitochondrial apoptotic genes (*CG3819* and *Aldh*) were upregulated, and negative regulators of apoptosis (*sens*, *eya*, *Pvf1*, *futsch*) were downregulated in both conditions. Also, cell survival genes such as *spitz*, an EGFR ligand, were downregulated. **B**) Strong dysregulation of cuticle proteins is observed in both *Gαq* overexpression and *Gαq* RNAi conditions. **C**) Ecdysone genes (*Blimp-1*, *lncRNA: let7c*) and nuclear hormone receptors (*Eip78c*, *Eip75b*, *Hr3*, *Hr4*) were downregulated. *Ftz-f1* and *ECR*, which are expressed in early larval stages, were upregulated. **D**) Heat map plot showing gene expression changes of the Insulin signaling components. *Pdk1* was downregulated in both *Gαq* O.E. and RNAi perturbations. Relaxin-like *dilp8* was significantly upregulated in both *Gαq* overexpression and RNAi conditions.

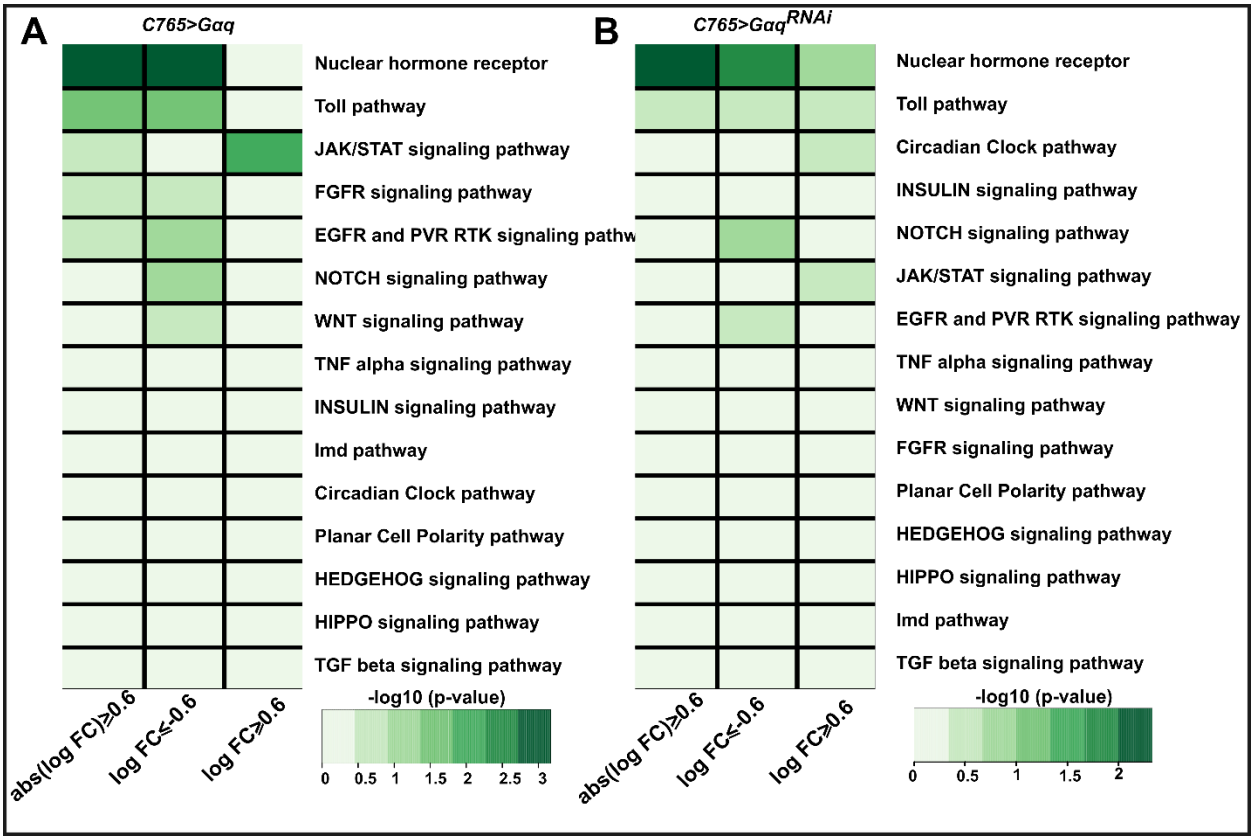


**Figure 7: Enrichment analysis of core signaling pathways among the differentially expressed genes. A**) Overexpression *Gαq* resulted in the enrichment of the Toll pathway and Nuclear hormone receptor among the differentially expressed genes with a significant fold change (abs (log2FC) ≥ 0.6)**.** Toll pathway and nuclear hormone receptor pathway were enriched among the genes that were significantly downregulated (log2FC ≤ -0.6). JAK/STAT signaling was enriched among the significantly upregulated genes (log2FC ≥ 0.6). **B**) For the *Gαq*$^{RNAi}$ perturbation, the nuclear hormone receptor pathway was enriched among the differentially expressed genes with a significant fold change (abs(log2FC) ≥ 0.6). Nuclear hormone receptor pathway was enriched among the significantly downregulated genes. No core signaling pathways were enriched among the significantly upregulated genes (log2FC ≤ -0.6).

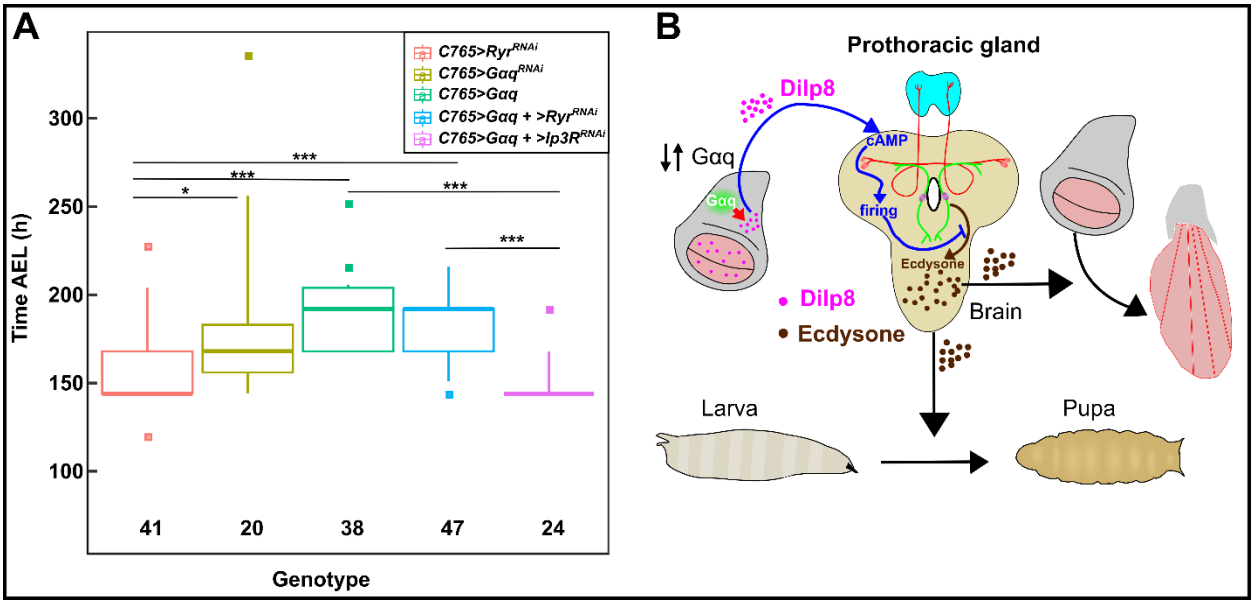


**Figure 8: Disruption of Gαq homeostasis delays larval to pupal transition. A**) A box plot illustrating the larval to pupal transition time for the genetic perturbations shown in the panel. Whiskers represent 5% and 95% percentiles. Square points represent the outliers. A Kruskhal-Wallis test revealed significant differences in pupariation times between the *Gαq* perturbations (the degrees of freedom is 4, the H is 62, and the p-value of $9.16 \times 10^{-13}$) (Degrees of freedom represents the number of groups subtracted with one. The test statistic H is compared with the critical value Chi-square for the given degrees of freedom). Conover post hoc test was used to perform multiple pairwise tests to compare the pupariation times between different genotypes. Asterisks indicate genotypes with statistically significant differences in pupariation times. Overexpression of *Gαq* delays larval to pupal transition by ~24 h, whereas $Gαq^{RNAi}$ delays transition time by ~12 h. Knockdown of $Ip_3R$ along with the *Gαq* overexpression rescues the developmental delay observed with *Gαq* overexpression. **B**) Proposed mechanism of developmental delay: Dysregulation of Gαq homeostasis in the wing disc upregulates *dilp-8* expression, ultimately resulting in decreased 20E synthesis from the brain. This generalization is consistent with RNA seq analysis from this work, where overexpression and downregulation of

1540 *Gαq* in the wing disc result in the downregulation of 20E target genes, respectively. Figure inspired

1541 from [157].